



Maximilian Neubauer, BSc

Experimental studies and modelling of reactive extraction in a Taylor-Couette-Disc-Contactor

Master Thesis

to achieve the university degree of
Diplom-Ingenieur
in
Chemical and Pharmaceutical Engineering

submitted to

Graz University of Technology

Supervisor:

Ass.Prof. Dipl.-Ing. Dr.techn. Susanne Lux
Institute of Chemical Engineering and Environmental Technology

Co-Supervisor:

Dipl.-Ing. Georg Rudelstorfer
Institute of Chemical Engineering and Environmental Technology

Graz, March 2021



Experimental studies and modelling of reactive extraction in a Taylor- Couette-Disc-Contactor

Maximilian Neubauer, BSc

Graz, March 2021

AFFIDAVIT

I declare that I have authored this thesis independently, that I have not used other than the declared sources/resources, and that I have explicitly indicated all material which has been quoted either literally or by content from the sources used. The text document uploaded to TUGRAZonline is identical to the present master's thesis.

16.03.2021

Date, Signature



Acknowledgement

At this point, I want to thank Ass.Prof. Susanne Lux and Dipl.-Ing. Georg Rudelstorfer for the excellent supervision of this thesis. Special thanks go to Georg Rudelstorfer, for his support and valuable input during every phase of this project, and not last for the freedom granted regarding working times and conduction of experiments. Furthermore, I want to thank the staff of the Institute of Chemical Engineering and Environmental Technology for support in various tasks as well as my colleagues at the institute for the good work atmosphere, which made experiments often running until late in the night much more pleasant. Finally, I want to thank my family and friends, particularly my parents and my sister for their unconditional support in every circumstance without which many things would have not been possible in the first place. Also, a big shout-out to Simone Santner for providing perfect lecture scripts throughout all the years of study.

Master thesis of Maximilian Neubauer

Experimental studies and modelling of reactive extraction in a Taylor-Couette-Disc-Contactor

Definition of task

In this work, experimental studies on the heterogeneous catalytic reactive extraction of acetic acid with methanol from aqueous feed solutions are to be conducted in a Taylor-Couette-Disc-Contactor. An existing plant used for the proof of concept is to be modified to improve validity of results. A chemical reaction engineering approach shall be used for modelling the concentration profiles of methanol, acetic acid and methyl acetate. These models shall then be used for a theoretical and exemplary scale up of the reactive extraction column.

Abstract

Experimental studies on the heterogeneous catalytic esterification of acetic acid with methanol with simultaneous solvent extraction of the reaction product with an isoparaffinic solvent from diluted aqueous feed solutions were conducted. The experiments were carried out in a Taylor-Couette-Disc-Contactor with an active height of 0.6 m and 50 mm in diameter. An already existing plant, which was used for the proof of concept in a previous work was modified. Models were used for description of concentration profiles. The aqueous phase was modelled as a continuous-stirred-tank-reactor cascade, with parameters retrieved from residence time distribution measurements. Model prediction was compared to experimental data. Regarding methyl acetate concentrations in the aqueous and organic phase, a simple model based on Nernst distribution was developed and compared to the experimental data. Exemplarily, a theoretical scale up of the reactor to an active height of 6 m was presented.

Kurzfassung

In dieser Arbeit wurde die heterogen katalytische Veresterung von Essigsäure mit Methanol, bei gleichzeitiger Extraktion des Reaktionsprodukts mit einem Isoparaffingemisch als Lösungsmittel, in verdünnten wässrigen Lösungen untersucht. Die Versuche wurden in einem Taylor-Couette-Disc-Contactor mit einer aktiven Höhe von 0,6 m und einem Durchmesser von 50 mm durchgeführt. Eine bereits bestehende Anlage, die in einer früheren Arbeit für ein Proof-of-concept verwendet wurde, wurde angepasst, um die Validität der generierten Daten zu erhöhen. Zur Beschreibung von Konzentrationsprofilen wurden Modelle verwendet. Die wässrige Phase wurde als kontinuierliche Rührkesselreaktorkaskade modelliert, wobei Parameter aus experimentellen Verweilzeitmessungen verwendet wurden. Für die Beschreibung der Methylacetatkonzentrationen in der wässrigen und organischen Phase wurde ein einfaches Modell basierend auf der Nernst-Verteilung entwickelt. Die Modellvorhersagen wurden anschließend mit den experimentellen Daten verglichen. Beispielhaft wurde ein theoretisches Scale-up des Reaktors auf eine aktive Höhe von 6 m vorgestellt.

Table of contents

Acknowledgement.....	IV
Definition of task.....	V
Abstract.....	VI
Kurzfassung	VII
List of symbols and abbreviations.....	X
List of figures.....	XII
List of tables	XV
1 Introduction and motivation	1
2 Theoretical Background	3
2.1 Process intensification	3
2.2 Extraction – Fundamentals and column types.....	5
2.2.1 Fundamentals	5
2.2.2 Extraction column types	7
2.3 Chemical reactions – kinetics and catalysis	11
2.3.1 Kinetics	11
2.3.2 Catalysis	12
2.4 Reactive Extraction – Fundamentals and Application in the TCDC	14
2.4.1 Fundamentals	14
2.4.2 Application of reactive extraction in the TCDC	14
3 Experimental Part	17
3.1 Chemicals and Equipment.....	17
3.1.1 Chemicals	17
3.1.2 Equipment.....	17
3.2 Conduction and development of experiments	18
3.2.1 Modified plant setup	18

Table of contents

3.2.2	Final experimental procedure	21
3.2.3	Plant modifications	23
3.2.4	Development of experimental procedure	26
3.2.5	Experimental matrix	30
4	Methods of data evaluation	31
4.1	Kinetics	31
4.2	Residence time distribution	32
4.3	CSTR-cascade modelling	33
4.3.1	Aqueous phase	33
4.3.2	Organic phase	34
4.4	Hold-Up	36
5	Results and discussion	37
5.1	General observations	37
5.2	Hold-up results	42
5.3	Influence of phase ratio on conversion	43
5.4	Molar process balances	44
5.5	Kinetic parameter fit	46
5.6	Residence time distribution	47
5.7	Modelling of the CSTR cascade	48
5.8	Modelling of methyl acetate concentrations	52
5.9	Scale up calculation	53
6	Summary and Outlook	57
7	Literature	59
8	Appendix	61
8.1	Pump calibration curves	61
8.2	Process Balances	62

List of symbols and abbreviations

Symbol/Abbreviation	Unit	Description
E_A	J mol^{-1}	activation energy
β	g l^{-1}	mass concentration
b.p.	$^{\circ}\text{C}$	boiling point
Bo	-	Bodenstein number
c	mol l^{-1}	molar concentration
D_{ax}	$\text{m}^2 \text{s}^{-1}$	axial dispersion coefficient
ΔH_r	kJ mol^{-1}	reaction enthalpy
ε	%	hold-up
E	s^{-1}	exit age
g	m s^{-2}	gravitational acceleration
Δh	m	height difference
K	-	distribution coefficient
k_1	$\text{l mol}^{-1} \text{s}^{-1}$	rate constant of forward reaction (reaction order $n = 2$)
k_2'	s^{-1}	rate constant of backward reaction (reaction order $n = 1$)
L	m	reactor length
N	-	number of vessels
P	-	phase ratio
dP	Pa	differential pressure
ΔP	Pa	hydrostatic pressure inside column
r	$\text{mol l}^{-1} \text{s}^{-1}$	reaction rate
ρ	kg m^{-3}	density
rpm	min^{-1}	rotational speed

σ_{θ}^2	-	dimensionless variance
T	°C	temperature
t	s	time
τ	s	residence time
u	m s ⁻¹	superficial velocity
V	m ³	volume
\dot{V}	m ³ s ⁻¹	volumetric flowrate
w_{cat}	%	catalyst weight fraction related to the flowrate of the aqueous phase
X	-	conversion

Superscript indices

a	aqueous
o	organic

Subscript indices

a	aqueous
cat	catalyst
HAc	acetic acid
H ₂ O	water
i	number of index
MeAc	methyl acetate
MeOH	methanol
o	organic
tot	total
0	inital

List of figures

Fig. 2-1: Principle of an extraction process [6].....	5
Fig. 2-2: Ternary diagram for a system where solvent extraction can be applied [6]...6	6
Fig. 2-3: Three types of static extraction columns [6].....	7
Fig. 2-4: Three types of pulsed extraction columns [6].....	8
Fig. 2-5: Selection of stirred extraction apparatuses [6]	9
Fig. 2-6: The TCDC results from the combination of a classical RDC design and the Taylor-Couette reactor (TCR) [11]	10
Fig. 2-7: Esterification of acetic acid with methanol under acidic catalysis yields methyl acetate and water.....	11
Fig. 2-8: Catalyzed and non-catalyzed reaction: comparison of the activation energy E_A (energy barrier) [21].....	12
Fig. 2-9: Steps involved during a heterogeneous catalytic reaction [25]	13
Fig. 2-10: Results of a reactive extraction experiment, top left: acetic acid concentration aqueous phase, top right: methanol concentration aqueous phase, bottom left: methyl acetate concentration organic phase, bottom right: methyl acetate concentration organic phase, [3].....	16
Fig. 3-1: Perforated rotor disc [3].....	19
Fig. 3-2: Modified plant used for reactive extraction experiments.	19
Fig. 3-3: P&ID of reactive extraction plant	20
Fig. 3-4: Left: conductivity sensor positioned at bottom of column. Right: Tracer injection port.....	23
Fig. 3-5: Flow breaker in upside down position, with septum inlet. Baffles made from stainless steel.....	24
Fig. 3-6: Feed preheater, insulated with ArmaFlex® in black.....	24

Fig. 3-7: Gas-liquid separator inside the organic phase outlet	25
Fig. 3-8: Left: T-piece, Right: Close up view of the inlet for pressure and temperature sensor as well as sample port	26
Fig. 3-9: Dampening elements for the differential pressure sensor. Left: rubber element marked in green. Right: Flexible connection to column head.....	26
Fig. 3-10: Left: Column head sealed with PE-foil, Right: Air cooler at high point of rising pipe, fabric tube with wrapped plastic net inside.....	27
Fig. 3-11: Comparison of methyl acetate concentrations in the ingoing aqueous streams for unsealed and sealed system. Parameters for both experiments: $T = 65\text{ }^{\circ}\text{C}$ $P = 1$ $\text{rpm} = 500$, data point connection by simple interpolation for trend visualization, $V_a=0.1\text{ l/min}$, $V_o=0.11\text{ l/min}$	28
Fig. 3-12: Comparison of acetic acid conversion for unsealed and sealed system over selected timeframe. Parameters for both experiments: $T = 65\text{ }^{\circ}\text{C}$ $P = 1$ $\text{rpm} = 500$, data point connection by simple interpolation for trend visualization, $V_a=0.1\text{ l/min}$, $V_o=0.11\text{ l/min}$	29
Fig. 4-1: Graphical representation of Eq. 11, with the 2 roots marked. Exemplary case ($X_i = 0.018$).....	34
Fig. 5-1: 3-phase flow (liquid-liquid-solid) in the TCDC, system: aqueous/organic/catalyst, photo taken with slow motion camera, $P=1$, $\text{rpm}=650$, $w_{cat} = 10.3\%$	37
Fig. 5-2: Differential pressure profile of reactive extraction process, mean value of 3 experiments (MN_07, MN_08, MN_09). Parameters: $T = 65\text{ }^{\circ}\text{C}$, $P = 0.5$, $\text{rpm} = 600$	38
Fig. 5-3: Methyl acetate concentrations in the aqueous phase	39
Fig. 5-4: Methyl acetate concentrations in the organic phase	39
Fig. 5-5: Methanol concentrations in the aqueous phase.....	40
Fig. 5-6: Methanol concentrations in the organic phase.....	40

Fig. 5-7: Acetic acid concentrations in the aqueous phase	41
Fig. 5-8: Acetic acid concentrations in the organic phase	41
Fig. 5-9: Comparison of conversion with varying phase ratios at 65°C, $P=\infty$ --> no extraction, only reaction	43
Fig. 5-10: Batch results of reactive extraction at 80°C (system: acetic acid / methanol / Shellsol T) by Maier [3], y-axis: acetic acid conversion, x-axis: time in hours, orange: $P=0.5$, green: $P=1$, blue: $P=2$, red: $P=\infty$	44
Fig. 5-11: Fit of Eq.5 for rate constants k_1 and k_2' to experimental data (mean values of MN_07, MN_08 and MN_09).....	46
Fig. 5-12: Comparison of experimental data with cascade model	47
Fig. 5-13: Regressed methanol concentrations in the aqueous phase.....	48
Fig. 5-14: Comparison of cascade model with regressed values	49
Fig. 5-15: Cascade model with extended kinetic equation	51
Fig. 5-16: Comparison of methyl acetate concentrations in the aqueous phase, model parameters: $K = 0.95$, $P = 0.5$	52
Fig. 5-17: Comparison of methyl acetate concentrations in the organic phase, model parameters: $K = 0.95$, $P = 0.5$	53
Fig. 5-18: Predicted acetic acid concentrations for scaled up process.....	55
Fig. 5-19: Predicted methyl acetate concentrations for scaled up process	55
Fig. 8-1: Pump calibration curves	61

List of tables

Table 1: Summary of selected definitions of process intensification by Van Gerven and Stankiewicz [4]	3
Table 2: Reactor parameters	18
Table 3: Experimental Matrix	30
Table 4: Hold-up values for organic phase and catalyst	42
Table 5: Molar process balance MN_09 (T = 65 °C, P = 0.5, rpm = 600).....	45
Table 6: Summary and results of the kinetic parameter fit for acetic acid conversion.	47
Table 7: parameters for scaled up reactor	54

1 Introduction and motivation

In view of the greenhouse gas problem, using biobased feedstock as resource for bulk chemicals is achieving increasing attention, with particular interest on the pulping industry, where currently about 50% of the wood processed is used to produce steam in the end. Potential valuable bulk products are lost in this process. Recovering these products instead of utilizing the side streams thermally is a topic of ongoing research. A challenge that comes with this effort is the often highly dilute nature of these aqueous multi component side streams, exhibiting in many cases complex vapour-liquid equilibria. This leads to energy-intensive downstream processing for conventional processes. In addition to that, simple rectification is often not feasible at all. Formic acid and acetic acid, which are among the main constituents of effluents that arise from pulp and paper production, are important bulk chemicals in a wide variety of branches, ranging from food over textile industry to pharmaceutical production [1]. Both acetic acid and formic acid are found in the black liquor, which is a by-product of the Kraft pulping process containing inorganic chemicals used in the pulping process and combustible organic material [2]. If heat is to be produced from the dilute black liquor, it has to be concentrated. The aqueous condensate of the evaporators contains the main amount of the low molecular weight carboxylic acids. Recovering these compounds from the dilute condensate is of interest because of the compounds themselves being valuable bulk products as well as lowering the biochemical oxygen demand for wastewater treatment. As mentioned above, conventional downstream processing comes along with an energy demand too high for the profitability of such a process. Therefore, alternative ways of recovering low molecular weight carboxylic acids from dilute aqueous feed streams are needed. Chemical conversion coupled with physical extraction may prove a viable candidate, while a prerequisite for an application at the technical scale is a continuous process. This idea was developed for the heterogeneous catalytic esterification with simultaneous solvent extraction. For the continuous process, the application in a Taylor-Couette-Disc-Contactor (TCDC) is a promising option. From the hydrodynamic standpoint, this novel extractor type developed at TU Graz is a hybrid between the Taylor-Couette reactor and the classical Rotating-Disc-Contactor. It has been shown that the TCDC is able to handle 3-phase liquid-liquid-

solid flow, a prerequisite for esterification via heterogeneous catalysis with simultaneous solvent extraction of the product [1]. Further research by Maier focused on the kinetics of the heterogeneous catalytic esterification of acetic acid with methanol and simultaneous extraction of the reaction product methyl acetate. Applicability of this process in a laboratory scale TCDC was also shown [3]. Since the proof of concept for heterogeneous catalytic esterification of acetic acid with methanol and simultaneous extraction of the reaction product in a TCDC was made, further research is needed for a deeper understanding of this process. No models are yet available to describe to concentration profiles of involved compounds inside the reactor. However, such models are critical for scale up predictions. In this work, the existing process and experimental procedure are developed further to improve validity of experimental results. Finally, models are developed and compared to the experimental data.

2 Theoretical Background

In the theoretical part of this thesis, the concept of process intensification, the fundamentals of extraction and chemical reactions, as well as the process of reactive extraction is described. Furthermore, the current state of research regarding reactive separations in the Taylor-Couette-Disc-Contactor (TCDC) is discussed.

2.1 Process intensification

Process intensification is one of the most promising and fastest growing fields in the chemical process industry. Yet there does not exist a general definition which is agreed upon and various definitions have emerged over the years [4,5]. A summary by Van Gerven and Stankiewicz of the existing definitions is shown in Table 1 below.

Table 1: Summary of selected definitions of process intensification by Van Gerven and Stankiewicz [4]

Process Intensification	Reference
"[is the] devising exceedingly compact plant which reduces both the 'main plant item' and the installations costs."	Ramshaw (1983)
"[is the] strategy of reducing the size of chemical plant needed to achieve a given production objective."	Cross and Ramshaw (1986)
"[is the] development of innovative apparatuses and techniques that offer drastic improvements in chemical manufacturing and processing, substantially decreasing equipment volume, energy consumption, or waste formation, and ultimately leading to cheaper, safer, sustainable technologies."	Stankiewicz and Moulijn (2000)
"refers to technologies that replace large, expensive, energy-intensive equipment or processes with ones that are smaller, less costly, more efficient or that combine multiple operations into fewer devices (or a single apparatus)."	Tsouris and Porcelli (2003)
"provides radically innovative principles ("paradigm shift") in process and equipment design which can benefit (often with more than a factor two) process and chain efficiency, capital and operating expenses, quality, wastes, process safety and more."	European Roadmap for Process Intensification (2007)
"stands for an integrated approach for process and product innovation in chemical research and development, and chemical engineering in order to sustain profitability even in the presence of increasing uncertainties."	Becht et al. (2008)

2 Theoretical Background

As all the various definitions cannot be discussed in detail here, one more recent approach by Van Gerven and Stankiewicz shall be outlined. Van Gerven and Stankiewicz have proposed a more comprehensive and fundamental vision on process intensification in their review paper from 2009 [4]. Four guiding principles have been provided.

- Maximization of the effectiveness of intra-and intermolecular events
- Provide the same processing experience for each molecule
- Optimization of driving forces at each scale and maximization of the surface area to which these driving forces apply to
- Maximization of synergistic effects between partial process steps

A summary of this approach by Van Gerven and Stankiewicz has been provided by Keil [5], and shall be explained in this paragraph. The first point refers to the molecular scale. Modifications can be realized regarding chemical routes, kinetics, or topology of the catalyst support. Here, process intensification is connected closely to the field of catalysis. Achieving the second principle may be accomplished using static mixers for example, which enable mixing while also maintaining almost ideal plug flow behaviour. Another example is gradientless and uniform heating of plug flow reactors, which can be reached by utilizing microwave technology. The third principle is dealing with enhanced heat and mass transfer. Examples are membrane reactors and multiphase flow reactors with phase-transfer catalysis supported by ultrasound. Higher mass transfer rates can also be achieved due to shorter diffusion paths in micro reactors and optimized pore structures. Another example brought up by Keil is the oscillating mode of operation in bubble columns, trickle-flow reactors, or reversed flow of mass and/or heat in plug flow reactors, which can increase rates of catalytic reactions. The fourth and last point refers to the utilization of multifunctional apparatuses at the macro scale, with one of the most prominent examples being reactive distillation. Here, chemical reaction and thermal separation are combined to obtain higher yields via removal of the reaction product.

2.2 Extraction – Fundamentals and column types

The information in this section is mainly derived from the book “Thermische Verfahrenstechnik” by Mersmann et al. [6].

2.2.1 Fundamentals

Extraction describes the process of the separation of compounds under the use of a liquid solvent from liquid respectively solid mixtures. While separation of compounds from liquids with a solvent is known as liquid-liquid or solvent extraction, separation of compounds from solids with a liquid solvent is known as solid-liquid extraction or leaching. Prerequisite for an extraction process is, that the liquid solvent does not or just partially mix with the carrier. A miscibility gap has to exist so that mass transfer between phases can occur. The carrier phase is also called raffinate phase, while the solvent phase is also denoted as extract phase.

The principle of an extraction process is shown in Fig. 2-1 below. In the extractor, the feed is brought into contact with the solvent, so that mass transfer can take place between the phases. Afterwards, the phases are separated, and the concentration of the compound of interest in the raffinate phase is now lower than in the feed stream. In a regenerator, the compounds transferred from the raffinate phase to the extract phase are separated from the solvent. The recycled solvent is then again fed to the extractor.

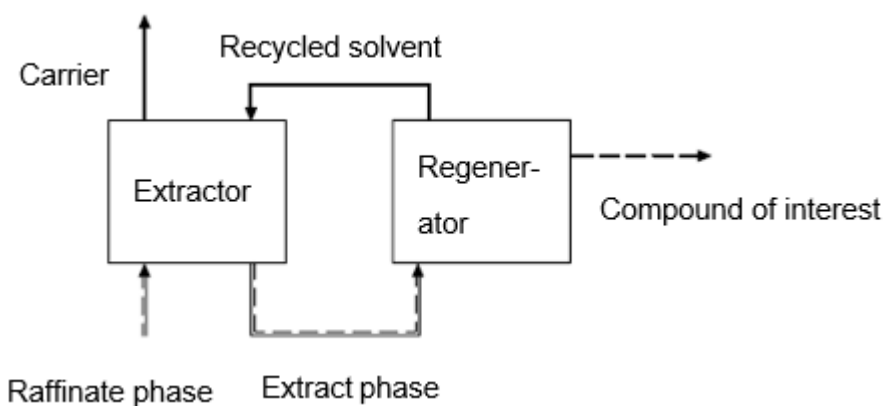


Fig. 2-1: Principle of an extraction process [6]

As mentioned before, a prerequisite for extraction is a sufficiently large miscibility gap between raffinate and extract phase. Fig. 2-2 shows the ternary diagram of a system,

2 Theoretical Background

where solvent extraction is applicable. A broad miscibility gap exists between carrier and solvent. For rising amounts of compound B, this gap narrows down and eventually vanishes. The binodal curve sets the limits for the miscibility gap in the diagram. Inside the miscibility gap, the connodes connect equilibrium states of raffinate and extract phase, meaning that a mixture inside the miscibility gap will separate along a connode into two phases. For interpolation between connodes, an auxiliary line is delineated in the diagram.

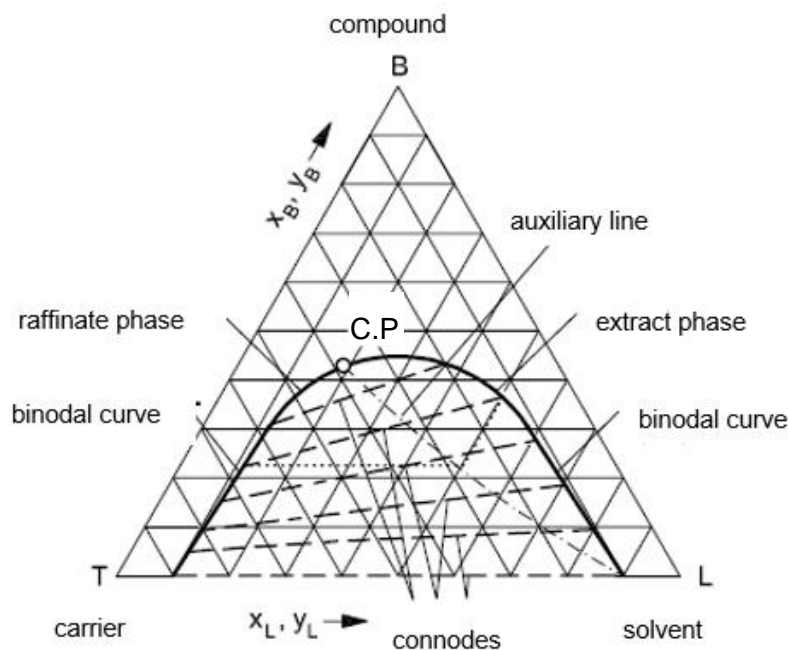


Fig. 2-2: Ternary diagram for a system where solvent extraction can be applied [6]

The equilibrium states of both phases approach each other as amount of compound B increases. Density difference and difference in interfacial tension decrease and become zero at the critical point. Extraction in the vicinity of the critical point is not feasible, since very low interfacial tension results in very small droplet size, which makes separation difficult to impossible.

Of great importance is the choice of the solvent for an extraction process. Distinct miscibility gap, selectivity and capacity in regard to the compound to be extracted, chemical stability, low toxicity and low price are some of the most important parameters to be considered when choosing a solvent for the process.

2.2.2 Extraction column types

A wide variety of designs for extraction columns exists and a basic classification into three types can be made; static columns (without energy input), pulsed columns and stirred columns. The focus in this section, however, is laid on the Taylor-Couette-Disc-Contactor as this apparatus is also used in the experimental part of this thesis.

Static columns

Three of the most common types of static columns are shown in Fig. 2-3 below.

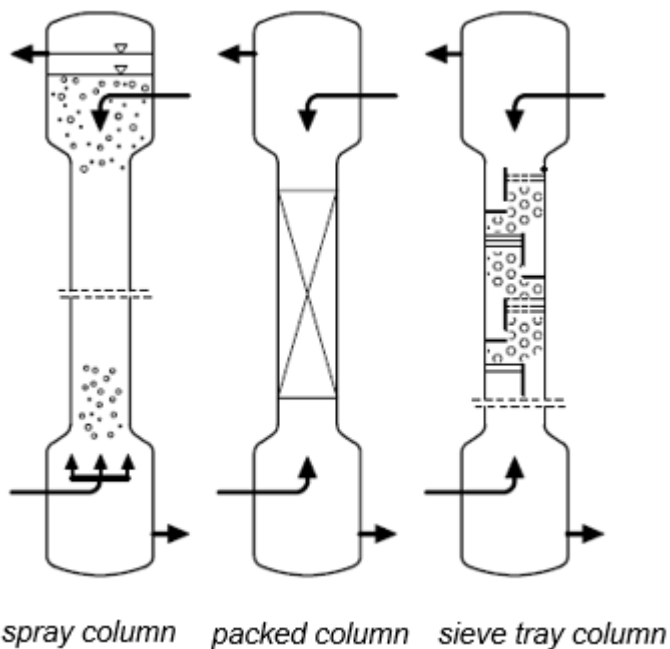


Fig. 2-3: Three types of static extraction columns [6]

In the spray column, no internals are present. The dispersed phase moves against the continuous phase in counter-current flow. A spray column is only feasible, if there is a difference in density of more than 150 kg/m^3 and the needed mass transfer performance is low. Because of the low separation efficiency, spray columns are utilized rather seldom. The second type is the static packed column, where the design is very similar to packed columns for rectification or absorption [6]. In contrast to rectification or absorption, the function of the packings in liquid-liquid extraction is an increase in residence time for the dispersed phase rather than increase of the mass transfer area, which in liquid-liquid-extraction columns is nearly independent of the packing surface

[7]. Thirdly, there is the sieve tray column. Here, the design differs from sieve tray columns for gas-liquid systems, as the sieve tray holes as well as the free relative hole area are smaller [6].

Pulsed Columns

Another class of extraction apparatuses are pulsed columns. Fig. 2-4 depicts three types of pulsed columns.

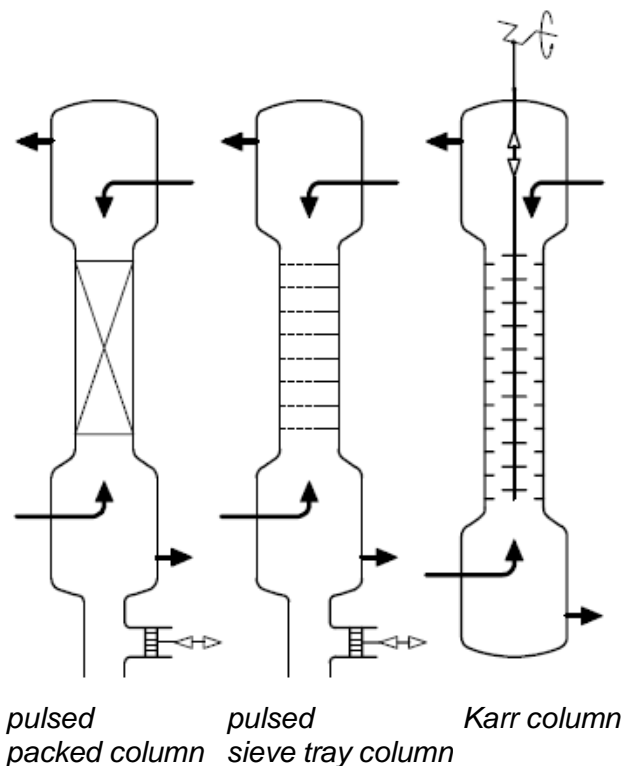


Fig. 2-4: Three types of pulsed extraction columns [6]

For the pulsed packed column and the pulsed sieve tray column, the liquid content of the column is moved up and down periodically with a certain frequency. The height of pulsation is typically between 0.8 and 1.2 cm, with pulsation intensity in the range of 0.8 to 2.5 cm/s. Pulsation leads to smaller droplets, which enlarges the mass transfer area and thus mass transfer itself. In the Karr column, pulsation of the liquid is realized by an eccentric drive, which moves the trays of the column in a periodical manner.

Stirred Apparatuses

The group of stirred apparatuses uses rotating internals to realize phase dispersion. A selection of common designs is depicted in Fig. 2-5 below.

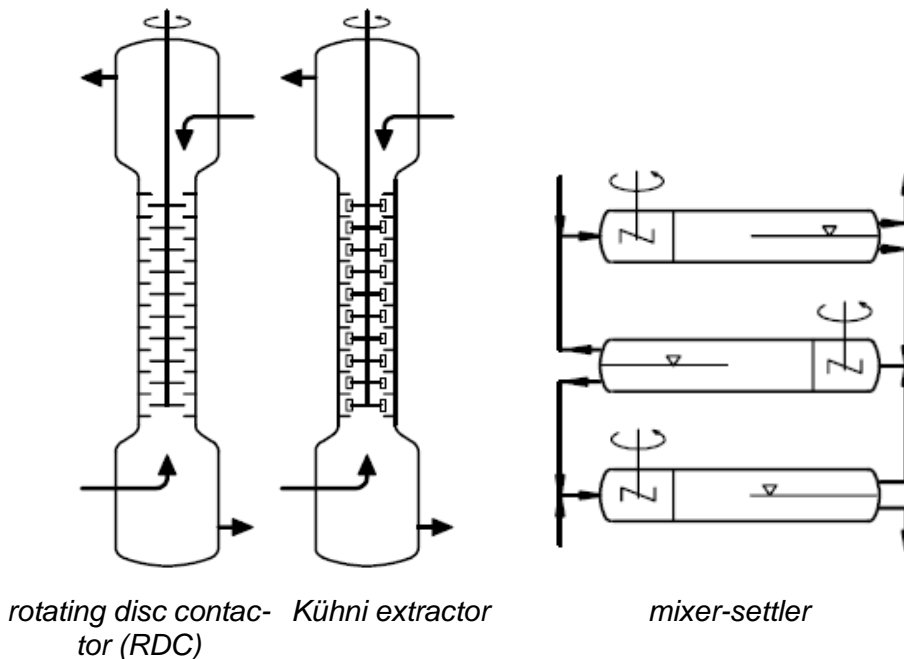


Fig. 2-5: Selection of stirred extraction apparatuses [6]

In both the rotating disc contactor (RDC) and the Kühni extractor, a rotating shaft is used. The difference between the two designs is that in the RDC, discs installed on the shaft are used for dispersion, while in the Kühni extractor bladed stirrers are utilized. Stator rings are installed in both column types, which reduce unwanted axial dispersion. Another type of stirred apparatuses of importance is the mixer-settler, which is simple in operating and can also be built at very large scales. Both phases are dispersed in the mixing zone and afterwards separated in the settling zone. In one mixer-settler unit, phases are moving in co-current. However, a back-mixing free counter-current flow can be realized using several connected units in a cascade (depicted in Fig. 2-5 above) [6].

The Taylor-Couette-Disc-Contactor – a new type of stirred extraction column

The origins of the Taylor-Couette-Disc-Contactor (TCDC) trace back to research regarding the optimization of existing and well-established rotating-disc-contactor columns. The result of the optimization was a novel apparatus design, which, from the hydrodynamic standpoint, is a hybrid between the rotating-disc-contactor and the Taylor-Couette reactor [8].

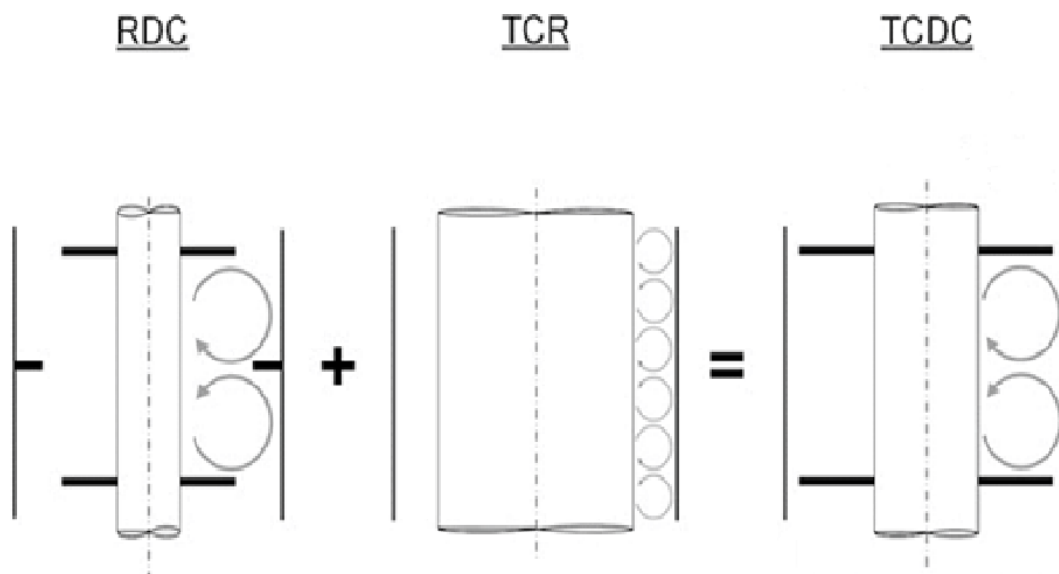


Fig. 2-6: The TCDC results from the combination of a classical RDC design and the Taylor-Couette reactor (TCR) [11]

As can be seen in Fig. 2-6 above, the stator rings have been abandoned completely and their function is replaced by rotor discs with larger diameter in the TCDC. This leads to optimized hydraulic parameters like droplet size distribution and axial back mixing. The abandonment of stator rings also makes the apparatus less susceptible to fouling, which is especially advantageous if feeds containing solid particles are processed. Also, manufacturing, cleaning and maintenance are facilitated with this design [8]. At this point, for more detailed information it shall be referred to the works of Aksamija and Graftschafter, who developed the Taylor-Couette-Disc-Contactor and conducted extensive research on its hydrodynamics [8,9,10,11].

2.3 Chemical reactions – kinetics and catalysis

In this chapter, the concept of reaction kinetics and catalysis will be briefly discussed. Special emphasis lays on the kinetics of the esterification of acetic acid with methanol with a heterogeneous catalyst.

2.3.1 Kinetics

The kinetics of a reaction describe, colloquially speaking, how fast a reaction is proceeding and are closely connected to the rate of reaction. Fogler defines the rate of reaction as “the number of moles of a compound reacting per unit time per unit volume” [12]. For purpose of clearness and because an esterification reaction was chosen as model reaction in the experimental part, further descriptions are based on the esterification reaction of acetic acid with methanol via heterogeneous catalysis. Extensive research has been conducted on this topic and kinetic data is available [13,14,15].

The reaction of carboxylic acids with alcohols under elimination of water is called esterification. The model reaction of acetic acid with methanol to yield methyl acetate under acidic catalysis is shown in Fig. 2-7 below.

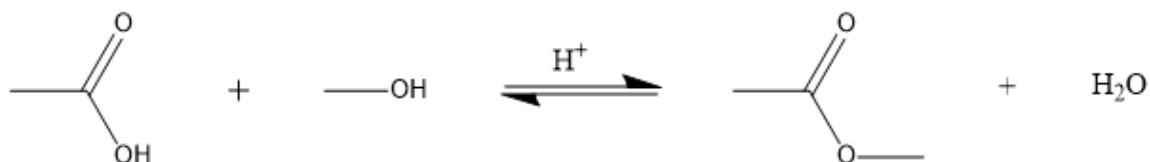


Fig. 2-7: Esterification of acetic acid with methanol under acidic catalysis yields methyl acetate and water

As the reaction arrow indicates, the esterification of acetic acid with methanol is an equilibrium reaction. However, the equilibrium can be shifted according to the principle of Le Chatelier, for instance by continuous removal of the product. This way, full conversion can be theoretically achieved.

2.3.2 Catalysis

A catalyst is a substance which increases the rate of a reaction while not being consumed by the reaction itself. The underlying principle is the lowering of the activation energy E_A . Two types of catalysis are distinguished: homogeneous and heterogeneous catalysis. In homogeneous catalysis, catalyst and reactants are present in the same phase. For heterogeneous catalysis, the opposite is the case, and catalyst and reactants are present in different phases, e.g., a solid catalyst in a liquid solution of reactants. For both types however, the same principle holds true – lowering of the energy barrier for the reaction. This principle is shown for a heterogeneous catalytic reaction in Fig. 2-8 below.

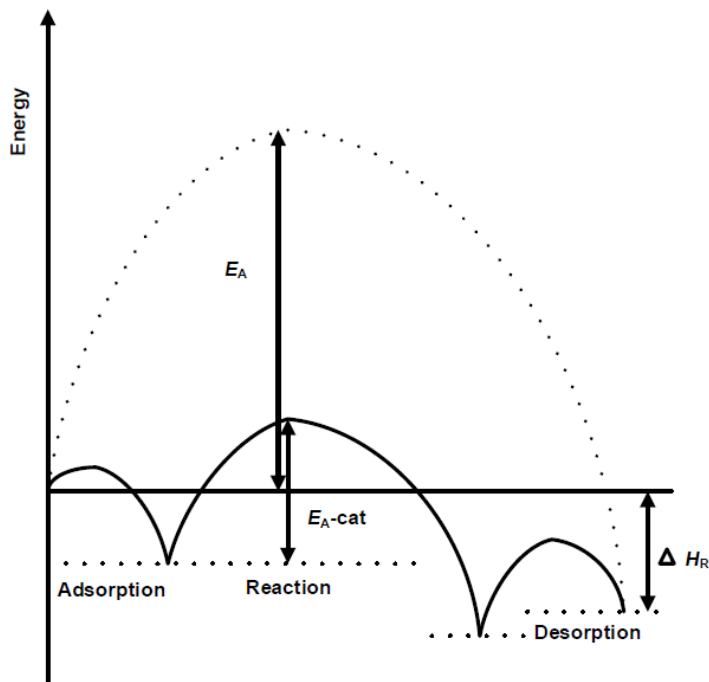


Fig. 2-8: Catalyzed and non-catalyzed reaction: comparison of the activation energy E_A (energy barrier) [21]

Reactants and products are involved in a series of steps during a heterogeneous catalytic reaction.

These steps are [16]:

1. Reactant diffusion across the boundary layer around the catalyst particle

2 Theoretical Background

2. Diffusion of the reactants to the active sites of the catalyst inside the pores
3. Adsorption of reactants on the active sites
4. Surface reaction, with formation or conversion of adsorbed intermediates involved
5. Desorption of the products from the sites of the catalyst
6. Diffusion of products through catalyst pores
7. Product diffusion through the boundary layer which surrounds the catalyst particle

A summary of the steps described is shown in Fig. 2-9 below.

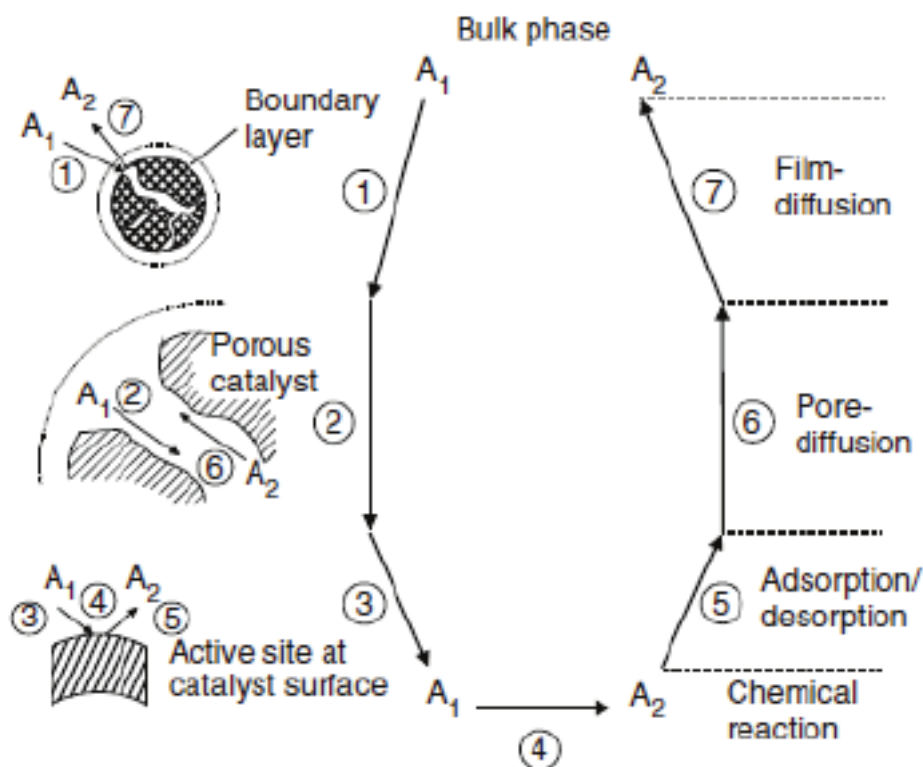


Fig. 2-9: Steps involved during a heterogeneous catalytic reaction [25]

2.4 Reactive Extraction – Fundamentals and Application in the TCDC

2.4.1 Fundamentals

Reactive Extraction is the combination of physical extraction and chemical reaction(s) in a single process unit [17]. In literature, mainly esterification is chosen as case study. Simulating reactive counter current extraction columns requires description of the reactive equilibria involved based on Gibbs excess models, knowledge of mass transfer and diffusion resistances, as well as a description of complex formation involving organic and aqueous species. Additionally, column hydrodynamics have to be considered [18].

Reactive extraction, like physical extraction, can be classified into liquid-liquid and solid-liquid extraction. In liquid-liquid reactive extraction, a solvent is added to the reaction system, which, in general, has high selectivity and miscibility regarding the products or intermediates of the reaction. That way, continuous removal from the reaction phase is possible. The solvent must be chemically inert and strongly immiscible towards the reactants, so that unwanted side reactions are avoided. By removing the products, further reactions and therefore also a yield reduction of the target compound are prevented [5].

2.4.2 Application of reactive extraction in the TCDC

The removal of carboxylic acids like acetic acid or formic acid from aqueous side streams in the pulping industry is subject of current research because of two main reasons. Firstly, these components are of interest as bulk chemicals widely used in different industries ranging from food industry to pharmaceutical production. Second, the wastewater treatment effort is reduced by lowering the biochemical oxygen demand. However, classical thermal separation operations like rectification are not feasible in this case, as the complex vapour-liquid equilibria of these mixtures exhibit azeotropic behaviour. Therefore, alternative separation processes are under investigation. Painer et al. proved the applicability of three-phase flow in the Taylor-Couette-Disc-Contactors. Two liquid phases, water and organic solvent, as well as a third, solid phase

2 Theoretical Background

in the form of solid catalyst particles form a stable multiphase flow in continuous operation [1].

Maier et al. further developed this concept and applied reactive extraction of acetic acid by esterification with methanol under heterogeneous catalysis at elevated temperatures in the TCDC. Experiments were conducted with an aqueous solution of 120 g/l acetic acid and an equimolar amount of methanol. Shellsol[®] T, a synthetical isoparaffinic hydrocarbon solvent, was used as extract phase. Experiments were conducted at 65 °C under heterogeneous catalysis with Amberlyst[®] 15, an acidic resin catalyst. The process was operated in circular, quasi-continuous mode, outgoing streams of the column were directed back into the feed tanks for respective phases. Operation however proved only possible with a fourth, gaseous phase, in this case air, added to the liquid-liquid-solid system. The introduction of an additional gaseous phase was made possible via a special rotor geometry, which was originally developed to tackle the problem of gas accumulation inside the compartments of the TCDC due to gassing out of the liquids at elevated temperatures. Samples were taken and analysed by titration and gas chromatography. Experimental duration was set for 4 hours [3].

Fig. 2-10 shows the results of one experiment. The enrichment of the extract phase with methyl acetate along the column as well as the decrease of methyl acetate in the aqueous phase along the column is visible. However, equilibrium has not been reached because of the duration of the experiment being just 4 hours. Nevertheless, the concept had been proven. Continuous reactive extraction of acetic acid with methanol via simultaneous physical extraction of its esterification product, methyl acetate, in a Taylor-Couette-Disc-Contactor is feasible [3].

2 Theoretical Background

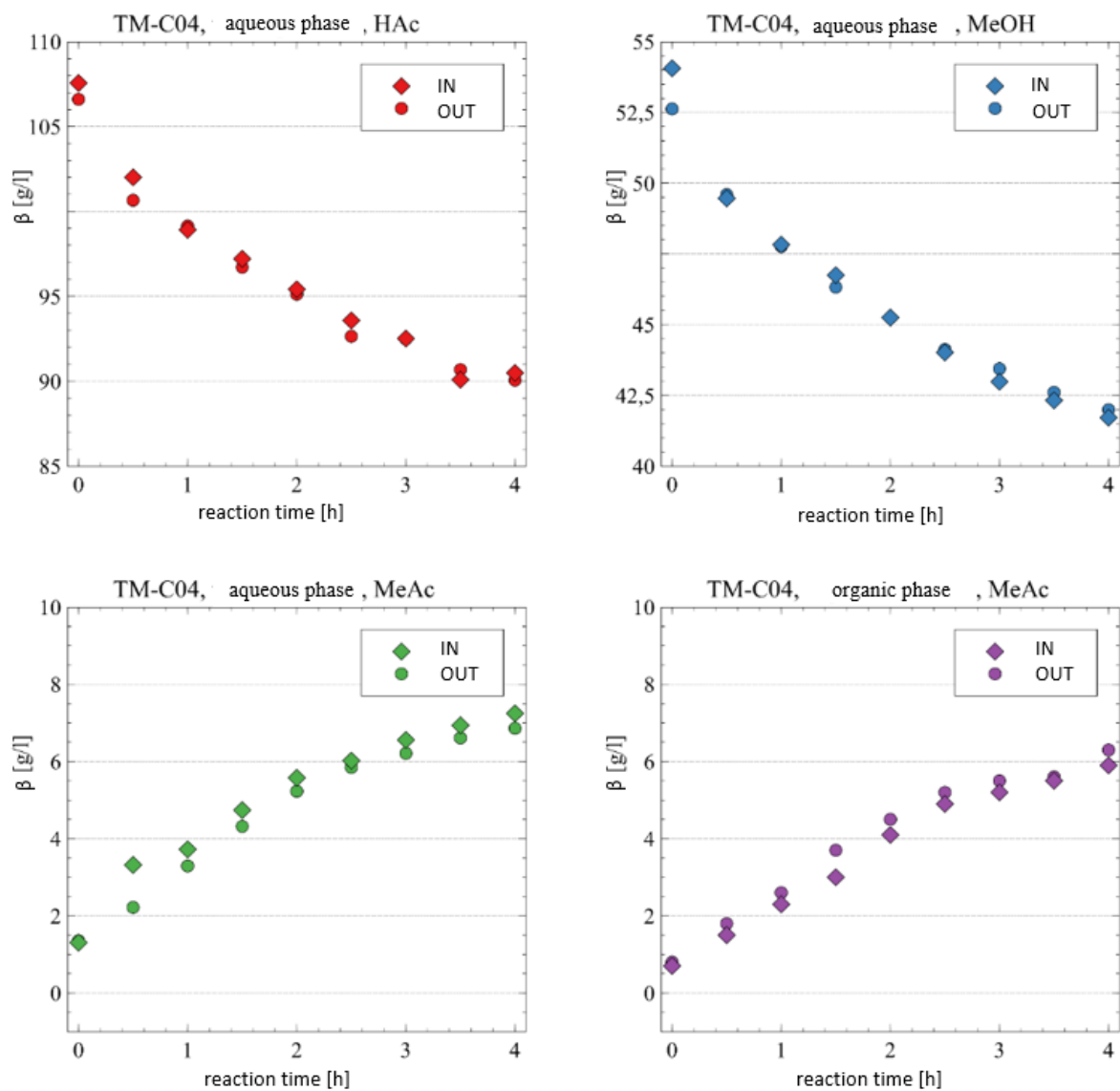


Fig. 2-10: Results of a reactive extraction experiment, top left: acetic acid concentration aqueous phase, top right: methanol concentration aqueous phase, bottom left: methyl acetate concentration organic phase, bottom right: methyl acetate concentration organic phase, [3]

3 Experimental Part

This part of the thesis covers the chemicals and equipment used and the development and conduction of experiments. Also, a summary of experiments in the form of an experimental matrix (Table 3) is provided.

3.1 Chemicals and Equipment

Chemicals and Equipment used in the experiments are listed in this section.

3.1.1 Chemicals

- Acetic Acid: Roth, 100%, CAS: 64-19-7
- Methanol: Roth, $\geq 99\%$, CAS: 67-56-1
- Amberlyst[®] 15: Sigma Aldrich, CAS: 39389-20-3
- Shellsol[®] T: Donauchem, CAS: 64741-65-7
- Deionized water: in-house source

3.1.2 Equipment

- Thermostats
 - Reactor double jacket: K20 Lauda, 2.2 kW
 - Feed preheater: Corio CD-200F, 2.0 kW
 - Storage tanks double jacket: Corio CP-601F, 2.0 kW
- Thermometer
 - Head: MGW Lauda R 42/2,
 - Bottom: MGW Lauda R 40/2,
- Pumps
 - Aqueous phase: Ismatec Ecoline VC-280
 - Organic phase: Ismatec Reglo Z (Pump head: Micropump[®] 81966 GJ-N21.FF2S.B)
 - Catalyst slurry: Ismatec Ecoline VC-280
- Stirrer: Hei-TORQUE Precision 200
- Differential pressure sensor: ICS Schneider Messtechnik, Type IDM 331

3 Experimental Part

- Gas Chromatography
 - Chromatograph: Shimadzu GC-2010 Plus, Autoinjector AOC-20i
 - Column: ZB-WAXplus
 - Detection type: FID

3.2 Conduction and development of experiments

The plant used for the reactive extraction experiments did not have to be constructed from scratch. As mentioned in the theoretical part, Maier already showed that reactive extraction in the Taylor-Couette-Disc-Contactor is feasible. However, some modifications of the existing plant had to be made to address some issues with the original design. Furthermore, the experimental procedure was adapted to increase the quality of outcome and the validity of data generated. For a better understanding, the final modified plant setup and final experimental procedure are described first. The modifications in detail are addressed after that.

3.2.1 Modified plant setup

Key parameters of the laboratory scale TCDC used for experiments are provided in Table 2 below.

Table 2: Reactor parameters

active length [mm]	600
reactor diameter [mm]	50
shaft diameter [mm]	25
number of compartments	24
compartment height [mm]	25
active volume [l]	0.88
rotor disc diameter [mm]	43
rotor disc geometry	perforated

3 Experimental Part

Fig. 3-1 shows the type of rotor disc used in the column.



Fig. 3-1: Perforated rotor disc [3]

The final setup of the plant is depicted below (Fig. 3-2), a P&ID is provided on the next page (Fig. 3-3).



Fig. 3-2: Modified plant used for reactive extraction experiments.

3 Experimental Part

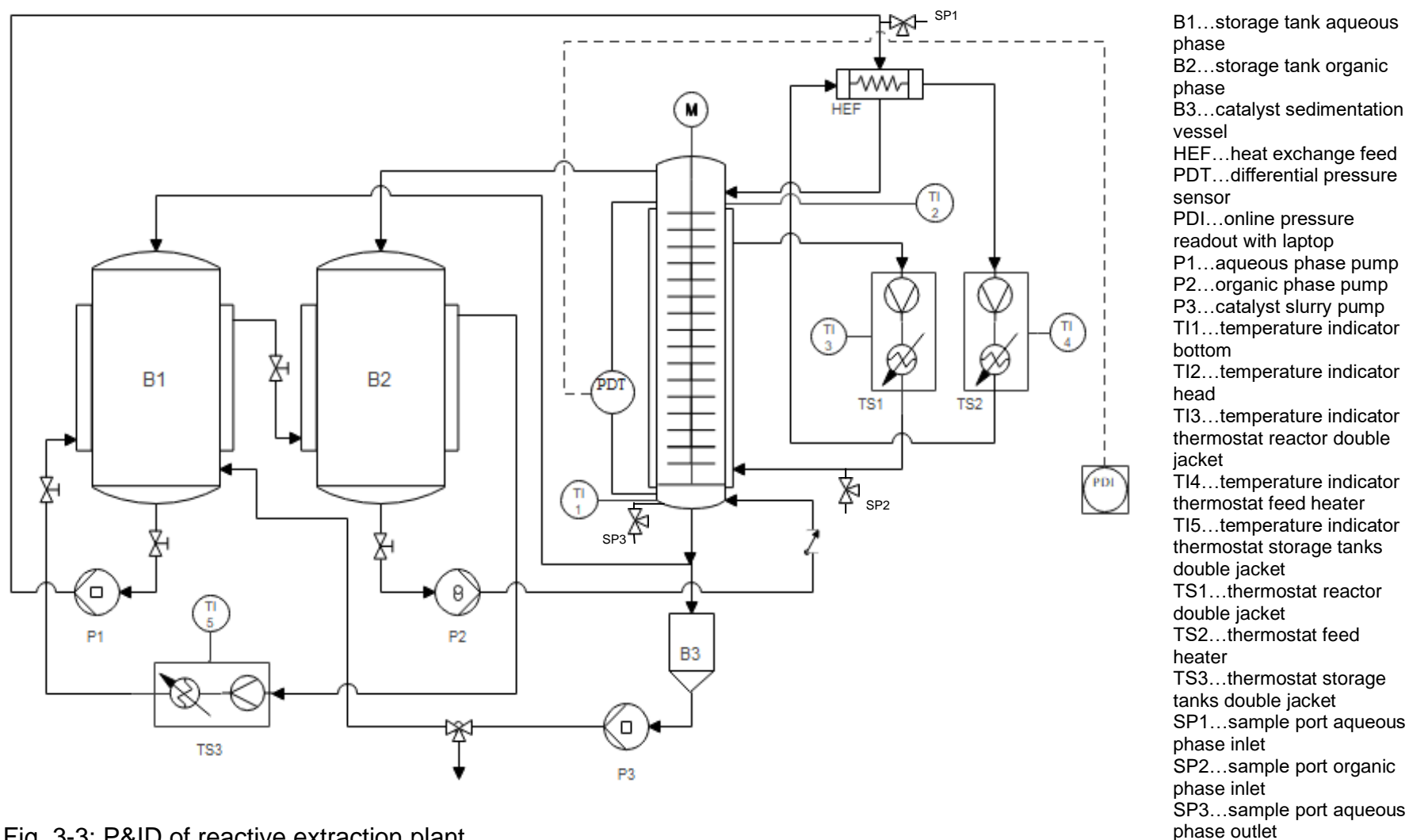


Fig. 3-3: P&ID of reactive extraction plant

3.2.2 Final experimental procedure

The final experimental procedure is described in this section. In the beginning, thermostats were set at temperature levels determined in pre-experiments to reach a process temperature of 65°C inside the column. The exact setting of the thermostats however varied between the experiments, depending on flow rates and temperature of surroundings, and had to be adjusted during the experiment as needed to maintain a constant temperature. For the preparation of the aqueous feed for all experiments, 480 g of acetic acid and 256 g of methanol were diluted with deionized water to a volume of 4 litres, resulting in a solution with mass concentrations of 120 g/l acetic acid and 64g/l methanol, corresponding to an equimolar solution of 2 mol/l for both compounds. Directly after preparation of the feed, a sample was taken.

All samples were taken with single use syringes, transferred into 1.5 ml crimp vials, which were capped and instantly put in an ice bath. Afterwards, they were stored in the temperature controlled autosampler (5 °C) of the GC. Samples were directly analysed without further dilution via split injection. Concentrations of acetic acid, methanol and methyl acetate in both phases were determined under the use of a FID.

The feed solution was transferred into the storage tank and aqueous phase circulation was started. Also, the organic phase tank was filled with according amounts of Shell-sol® T solvent, corresponding to the phase ratio of the experiment. By the time the upper bearing plate of the rotor shaft was covered with liquid, rotation was started. When temperatures had reached about 60 °C in column head and bottom, the organic phase pump was activated. The first sample was taken when a stable liquid-liquid flow in the column was reached. Next step was activation of the slurry pump for the catalyst. Stable liquid-liquid-solid flow was reached about 10 minutes after starting the slurry pump, and the second sample was taken. For the first 3 hours samples were taken every 30 minutes, after 3 hours in intervals of 1 hour. Each sampling procedure resulted in 4 samples: out-and ingoing stream for both aqueous and organic phase. Volumetric flow rates were set according to pump calibration curves, however manual validation of flow rates via weighing in a beaker was done to ensure the process was operating at correct parameters. If needed pump settings were adjusted accordingly.

3 Experimental Part

Liquid holdup measurements were performed with the differential pressure sensor, which also acted as a process control tool, for real time monitoring of the dispersed phase holdup.

Solid holdup of the catalyst was measured via markings on the settling tank. As reference zero, the height of the catalyst packing in the tank at the time of first particles arriving at the column head was chosen. First particles arriving at the packing defined the second marking. To validate this, the height of the catalyst bed shortly before the end of the experiment was marked. All pumps were turned off and the remaining catalyst particles in the column sedimenting down into the settling tank defined the second marking. After each run, the catalyst was removed from the column, washed 3 times with deionized water, and decanted. At 60 °C, the catalyst was stored in the drying chamber and used in the next but one experiment. Since the pumping of the slurry with a peristaltic pump led to grinding of the catalyst particles over the duration of the experiment, a certain amount had to be restocked by fresh catalyst. 140 g of dry catalyst were enough for one experiment. This amount was sufficient for a stable catalyst holdup inside the column while at the same time still forming a packed bed at the bottom of the sedimentation vessel. This was important as the flow resistance of the catalyst bed was needed to prevent the aqueous phase from being transported solely with the catalyst slurry. The loading of the column with recycled catalyst was always done after cleaning. For this purpose, the column was filled with deionized water. The dry catalyst was suspended in deionized water, decanted, and suspended again. This slurry was then poured into the column at the head, while the rotor was activated to ensure the sedimentation of all particles. After settling of the catalyst, the column was emptied of the liquid and ready for operation.

Residence time distribution (RTD) measurements were conducted with a pulse function set up. As tracer 1 ml of saturated sodium chloride solution was used, the exit age distribution was measured with a simple conductivity sensor. The tracer was injected

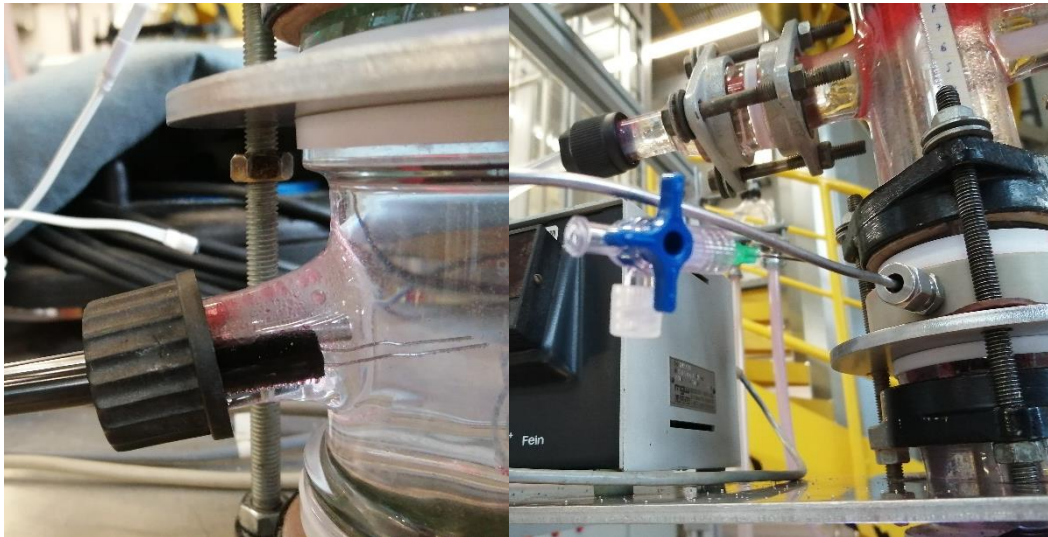


Fig. 3-4: Left: conductivity sensor positioned at bottom of column. Right: Tracer injection port

via the septum above the upper bearing plate (Fig. 3-4). The analysis of the RTD was done fully automatic by an already existing program implemented in LabView by Preisack [19]. Measurements were conducted at the operating points of reactive extraction experiments. However, RTD measurements for 3-phase flow (liquid-liquid-solid) could not be conducted due to the inherent operation principle of the plant. In 3 phase flow, aqueous phase loaded with tracer is also transported via the catalyst slurry and pumped back into the storage tank. Meaningful results are thus not achievable for 3-phase flow. Instead, for modelling, 2-phase flow measurements (liquid-liquid) were used, with the influence of the catalyst on the RTD assumed to be not significant.

3.2.3 Plant modifications

One of the main issues with the original plant was a temperature gradient inside the column in heated operation, with differences between column head and bottom up to 10 °C. To tackle this, a coil type preheater (Fig. 3-6) made of glass was installed before the feed inlet of the aqueous phase, with a separate thermostat for more flexible temperature control. All thermostats were operated with deionized water. Furthermore, for

3 Experimental Part

the heating of the storage tanks for aqueous and organic phase, a new thermostat was installed. A closer look on the fluid movement at the column head showed, that a spiral type flow around the rotating shaft reduced the upward movement of the dispersed phase and led to adverse flooding behaviour.

This problem was solved by installing an improvised and self-constructed flow breaker (Fig. 3-5), which was built in directly above the upper bearing plate, reducing the back-flow significantly.



Fig. 3-6: Feed preheater, insulated with ArmaFlex® in black.



Fig. 3-5: Flow breaker in upside down position, with septum inlet. Baffles made from stainless steel.

Other smaller modifications included the installation of a check valve in the connection between organic phase pump and organic phase inlet. This reduced the backflow of aqueous phase into the organic phase feed inlet when the organic phase pump was turned off. At the column head, in the outlet of the organic phase, a gas-liquid separator was installed (Fig. 3-7). The reason for this was discharge of aqueous phase into the organic phase tank when operating the column in gas-liquid-liquid mode, through ascending gas bubbles forming clusters with aqueous phase droplets. The separator,

3 Experimental Part

consisting of a thermally and chemically resistant folded polyethylene net, proved very effective in enabling a smooth gas-liquid-liquid operation.



Fig. 3-7: Gas-liquid separator inside the organic phase outlet

Another important part of the final setup used for reactive extraction experiments was the differential pressure sensor. This sensor was originally integrated into the plant by Liegl [20], who also wrote LabView programs for conduction of hold-up measurements. For the use of the sensor, a T-piece type adapter (Fig. 3-8) was installed at the bottom of the column, with two inlets: one for the organic phase and one for the sensor itself. The inlet for the pressure sensor was later modified to fit an additional temperature sensor and a 3-way sample port. Alternatively, the pressure sensor can be replaced with a conductivity sensor for residence time distribution measurements.



Fig. 3-8: Left: T-piece, Right: Close up view of the inlet for pressure and temperature sensor as well as sample port

Resonance vibrations of the plant at higher rotational speeds made it necessary to mount the sensor vibration damped (Fig. 3-9). Also, a new stirrer, with remote control via USB-cable and torque limiter, was incorporated.

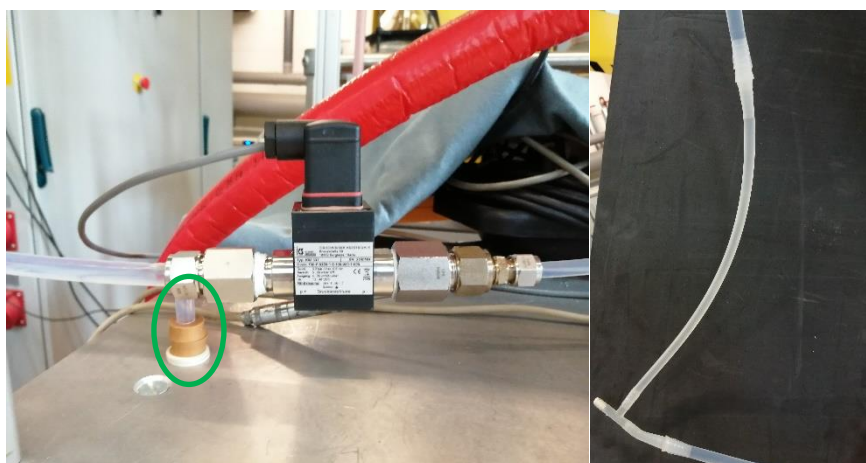


Fig. 3-9: Dampening elements for the differential pressure sensor. Left: rubber element marked in green. Right: Flexible connection to column head.

3.2.4 Development of experimental procedure

Before experiments with the reactive system, operating limits of the column were determined with the system water/Shellsol T[®]. The operating points of the reactive ex-

3 Experimental Part

traction experiments were then based on these pre-determined operating limits. Previous reactive extraction experiments by Maier were conducted over a fixed timeframe of 4 hours. However, after 4 hours equilibrium conversion was not yet reached. This was one of the main issues which was addressed in the beginning, with the first experiment having a duration of 6.5 hours, and the second one a duration of 10.5 hours. Still, no equilibrium conversion was reached, with a nearly linear increase in conversion after 4-5 hours (Fig. 3-12). The supposed reason for this was evaporation of the volatile components methyl acetate (b.p. 57.1 °C, atmospheric pressure) and methanol (b.p. 64.7 °C, atmospheric pressure) at process temperatures of 65°C. To tackle this problem, the plant was sealed from surroundings. Notable modifications are the sealing of the column head with polyethylene foil and the installation of an improvised air cooler at the high point of the rising pipe for the aqueous phase (Fig. 3-10).



Fig. 3-10: Left: Column head sealed with PE-foil, Right:
Air cooler at high point of rising pipe, fabric tube
with wrapped plastic net inside

3 Experimental Part

This approach proved successful, as in the next run, equilibrium was reached. Below, the comparison between sealed and unsealed system regarding methyl acetate concentration in the aqueous inlet stream at the column head and conversion of acetic acid is shown (Fig. 3-11, Fig. 3-12)

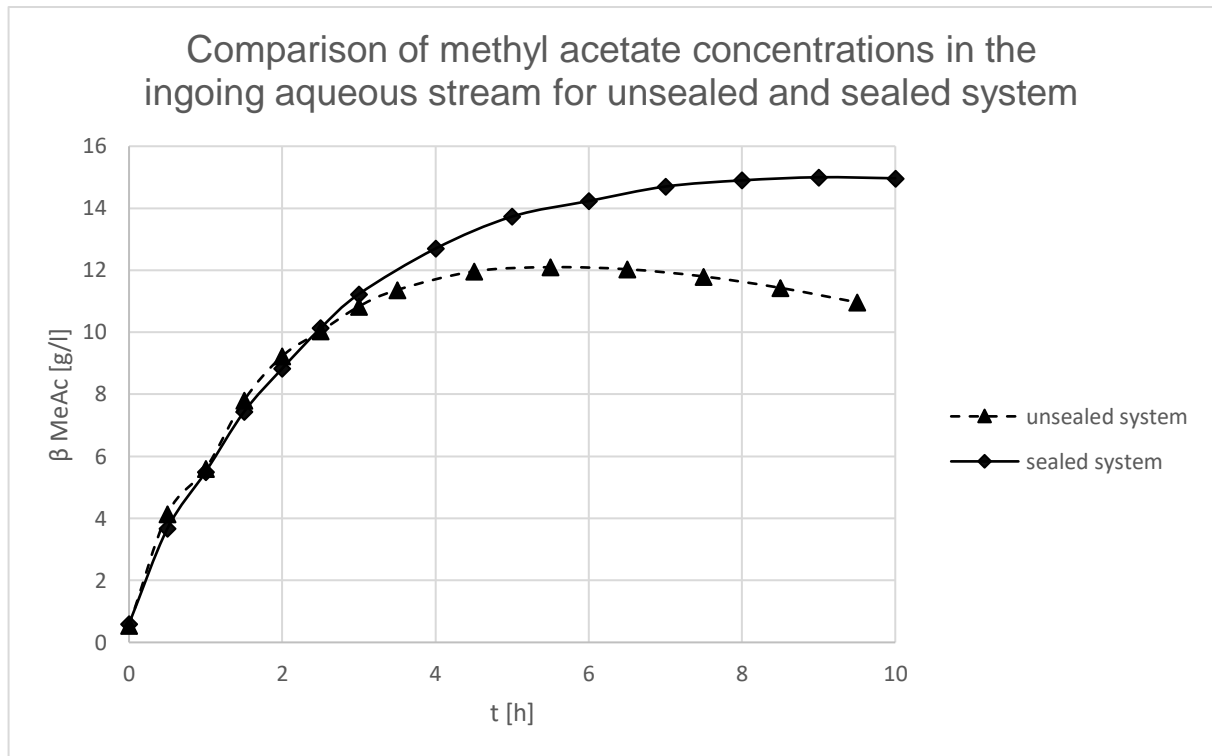


Fig. 3-11: Comparison of methyl acetate concentrations in the ingoing aqueous streams for unsealed and sealed system. Parameters for both experiments: $T = 65\text{ }^{\circ}\text{C}$ | $P = 1$ | $\text{rpm} = 500$, data point connection by simple interpolation for trend visualization, $\dot{V}_a = 0.1\text{ l/min}$, $\dot{V}_o = 0.11\text{ l/min}$

As can be seen above, for the first 3 hours of the experiments, the concentration profiles do not differ significantly. However, from 3 hours onwards, the difference becomes larger for increasing experiment duration. For the unsealed system, methyl acetate concentration even starts decreasing from 5.5 hours onwards. In the sealed system, equilibrium is reached, and concentration stays constant. Conversion profiles for acetic acid are shown in Fig. 3-12. According to the principle of Le Chatelier, by removal of the reaction product methyl acetate (in this case by evaporation) the equilibrium is constantly shifted to the product side and conversion increases. Equilibrium is not reached.

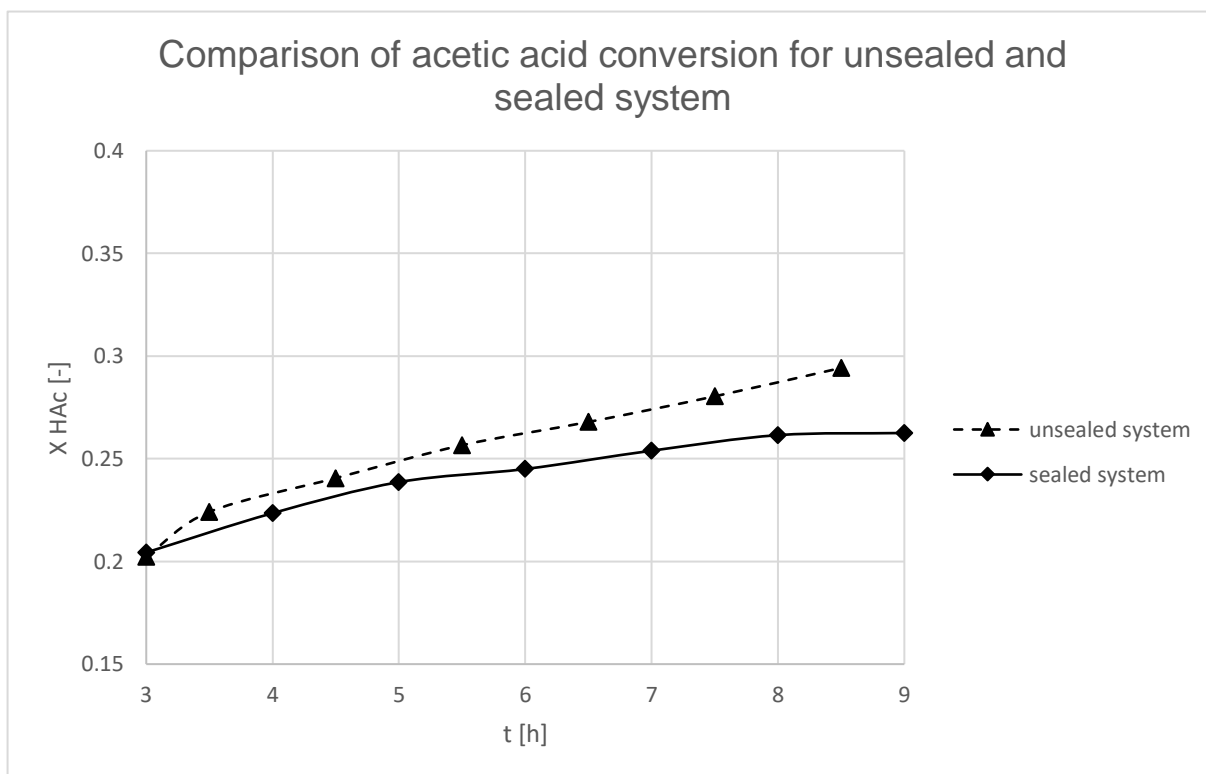


Fig. 3-12: Comparison of acetic acid conversion for unsealed and sealed system over selected timeframe. Parameters for both experiments: $T = 65 \text{ }^\circ\text{C}$ | $P = 1$ | rpm = 500, data point connection by simple interpolation for trend visualization, $\dot{V}_a = 0.1$ l/min, $\dot{V}_o = 0.11$ l/min

After the third experiment, new sampling methods were introduced to get a better representation of the actual change in concentrations along the column. For the organic phase outgoing stream, samples were not taken at the outlet but directly at the phase boundary in the column head, with a self-constructed sampling probe. This method eliminates errors related to concentration gradients in the settling zone above the phase boundary. For the aqueous phase outgoing stream, a new 3-way sample port, depicted in Fig. 3-8, was installed at the bottom of the column, reducing errors related to dead volumes in the settling tank for the catalyst and the rising pipe. For the aqueous ingoing stream, sampling was also tried directly at the column head, introducing a 3-way port into the septum where the upper temperature sensor is located. However, this method was discarded since small droplets of organic phase were drawn into the syringe when taking samples. Another novelty in the experimental procedure is, that the addition of air for stable operation is not necessary, reducing the complexity and effort from the apparatus point of view.

3 Experimental Part

3.2.5 Experimental matrix

Table 3: Experimental Matrix

	MN_01	MN_02	MN_03	MN_04	MN_05	MN_06	MN_07	MN_08	MN_09	MN_10
P [-]	0.5	1	1	2	1	0.5	0.5	0.5	0.5	0.5
T [°C]	65	65	65	65	65	65	65	65	65	65
rpm [1/min]	500	500	500	500	650	650	600	600	600	600
P1 [%]	8	8	8	8	8	5/6	5	5	5	5
P2 [%]	17	13	13	11	13	14	14	13	13	0
P3 [%]	3	3	3	3	3	3	2	2	2	2
\dot{V}_a [l/min] calibrated	0.1	0.1	0.1	0.1	0.1	0.06/0.07	0.06	0.06	0.06	0.06
\dot{V}_a [l/min] calibrated	0.2	0.11	0.11	0.09	0.09	0.13	0.13	0.11	0.11	0
\dot{V}_a [l/min] actual				0.1	0.1	0.056/0.069	0.051	0.054	0.55	0.051
\dot{V}_o [l/min] actual		0.095	0.1	0.046	0.046	0.108	0.096	0.099	0.099	0.096
Catalyst weight frac- tion [%]	10.3	10.3	10.3	10.3	10.3	11.5/13.8	11.5	11.5	11.5	11.5
Comment		Rerun MN_02 with sealed system				Increasing P1 by 1% during experi- ment, reason: no aqueous phase out- put through rising pipe, all liquid tran- ported by slurry phase	used for mod- elling	used for mod- elling	used for mod- elling	no extraction, only reaction

4 Methods of data evaluation

In this chapter the mathematical procedures for data analysis and modelling are explained. In short, the calculation sections are: retrieving of kinetic parameters from acetic acid conversion data, calculation of the number of vessels via residence time distribution and finally modelling of the concentration profiles of methanol and methyl acetate via a continuous-stirred-tank reactor (CSTR) cascade and a model based on the Nernst distribution law.

4.1 Kinetics

According to Maier [3], the kinetics of a pseudo-homogeneous second order reversible reaction for constant catalyst load can be described by

$$-r_{HAC} = -\frac{dc_{HAC}}{dt} = k_1 c_{HAC,0}^2 (1 - X)^2 - k_2' \frac{c_{HAC,0} X}{1 + K} \quad (\text{Eq.1})$$

This equation is valid for following assumptions

- Equimolar starting concentrations of acetic acid and methanol
- The system is treated as diluted, thus the concentration of water is approximately constant and is incorporated into rate constant k_2'
- Methyl acetate concentration follows the Nernst distribution law, which is also only valid for diluted systems
- The distribution coefficient K is treated as constant and non-dependent on the change in the composition of the phases during the process
- Ideal solution behaviour, concentrations are used instead of activities
- Acetic acid and methanol are not present in the organic phase in significant amounts

For fitting the equation to conversion/time data, rearrangements are made. Acetic acid concentration for conversion X is given by

$$c_{HAC} = c_{HAC,0} (1 - X) \quad (\text{Eq. 2})$$

with the derivative

$$dc_{HAc} = -c_{HAc,0}dX \quad (\text{Eq. 3})$$

Substitution of dc_{HAc} in Eq.1 yields

$$-c_{HAc,0} \frac{dX}{dt} = k_1 c_{HAc,0}^2 (1-X)^2 - k'_2 \frac{c_{HAc,0} X}{1+K} \quad (\text{Eq.4})$$

Which finally equates to

$$\frac{dX}{dt} = k_1 c_{HAc,0} (1-X) - k'_2 \frac{X}{1+K} \quad (\text{Eq. 5})$$

This differential equation can now be used for directly fitting the conversion/time data with parameters k_1 and k'_2 . Fitting of Eq. 5 was implemented in Wolfram Mathematica via a combination of a numerical ordinary differential equation solver and a nonlinear model fitting procedure.

4.2 Residence time distribution

Two variants for the determination of the number of vessels for the CSTR-cascade model have been applied. The first variant starts from the axial dispersion coefficient determined by RTD measurements. This parameter is calculated from experimental data via an already existing routine implemented in LabView. The Bodenstein number Bo is given as in [21] by

$$Bo = \frac{uL}{D_{ax}} \quad (\text{Eq. 6})$$

The number of vessels N can be calculated from the inverse of the dimensionless variance σ_θ^2 which is obtained for the open-open model (applicable because back mixing is not restricted to the system boundaries) as in [21] by

$$\sigma_\theta^2 = \frac{2}{Bo} + \frac{8}{Bo^2} = \frac{1}{N} \quad (\text{Eq. 7})$$

The second variant is a direct fit of the exit age distribution $E(t)$ to experimental RTD data with the parameter N corresponding to the number of vessels in the CSTR-cascade. The exit age distribution is given as in [21] by

$$E(t) = \frac{t^{N-1}}{(N-1)! \left(\frac{\tau}{N}\right)^N} e^{-N\frac{t}{\tau}} \quad (\text{Eq. 8})$$

4.3 CSTR-cascade modelling

4.3.1 Aqueous phase

The target is to find a model which describes the change in concentration for different initial concentrations over the length of the reactor, which corresponds to the difference between inlet and outlet. The kinetics are obtained according to section 3.1, from the conversion/time curve of acetic acid, since acetic acid (b.p. 118 °C, atmospheric pressure) is not a volatile compound at a process temperature of 65 °C and can thus be treated as a stable reference. The number of vessels is derived like described in section 3.2.

For CSTR i in a cascade of N CSTRs following equation for the residence time τ according to [21] can be applied

$$\tau_i = \frac{\tau_{tot}}{N} = \frac{c_{A,0}(X_i - X_{i-1})}{-r_i} \quad (\text{Eq. 9})$$

Which in the specific case corresponds to

$$\tau_i = \frac{\tau_{tot}}{N} = \frac{c_{HAc,0}(X_i - X_{i-1})}{k_1 c_{HAc,0}^2 (1 - X_i)^2 - k_2' \frac{c_{HAc,0} X_i}{1+K}} \quad (\text{Eq. 10})$$

The calculation of conversion X_N after N vessels is done iteratively by solving Eq. 9 numerically for different starting values of $c_{HAc,0}$ and $c_{MeOH,0}$. This is done by rearranging Eq. 10 for

$$0 = \frac{c_{HAc,0}(X_i - X_{i-1})}{k_1 c_{HAc,0}^2 (1 - X_i)^2 - k_2' \frac{c_{HAc,0} X_i}{1+K}} - \tau_i \quad (\text{Eq. 11})$$

and searching for the roots. Eq. 11 has two roots, which was checked graphically. One of them is X_i , which lies in the only meaningful range between 0 and the equilibrium conversion. The root finding routine was performed in Matlab®.

In practice, it emerged that using a positive starting value close to zero (0.0001) returned the root of the function in the meaningful range.

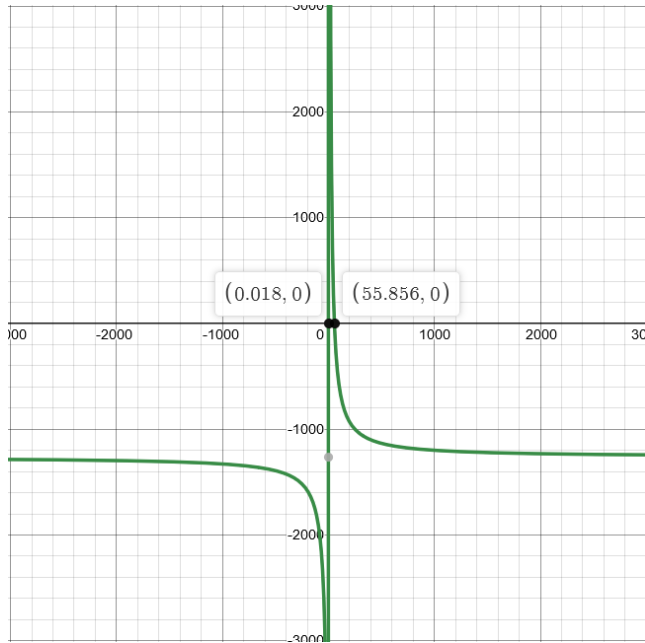


Fig. 4-1: Graphical representation of Eq. 11, with the 2 roots marked. Exemplary case ($X_i = 0.018$)

The obtained values for X_i are then used for the calculation of X_{i+1} . As starting values for acetic acid and methanol concentrations respectively, values from polynomial regression of experimental data are used. The starting values represent the inlet concentration. The outlet concentration according to the model is then obtained by

$$c_{HAc,N} = c_{HAc,0}(1 - X_N) \quad (\text{Eq. 12})$$

The outlet concentration according to the model is then compared to regressed outlet concentrations from experimental data.

4.3.2 Organic phase

For modelling the concentration profiles in the organic phase, the cascade model cannot be used directly since methyl acetate concentrations in respective phases are following distribution laws rather than kinetics.

A simple model based on Nernst distribution was developed to describe concentration profiles for methyl acetate in aqueous and organic phase. The Nernst distribution law

4 Methods of data evaluation

is valid for non-miscible phases and diluted systems, which holds true for the reported system in good approximation.

Starting point was the definition of the distribution coefficient K

$$K = \frac{c_i^\beta}{c_i^\alpha} \quad (\text{Eq. 13})$$

which in the specific case corresponds to

$$K = \frac{c_{MeAc}^o}{c_{MeAc}^a} \quad (\text{Eq. 14})$$

The reactive extraction process is treated as single stage extraction in this model. For the extraction process the total molar sum of target compound in both phases before and after the extraction is constant

$$n_{tot} = const \quad (\text{Eq. 15})$$

This can be expanded into

$$c_{MeAc,0}^a V_0^a + c_{MeAc,0}^o V_0^o = c_{MeAc,1}^a V_1^a + c_{MeAc,1}^o V_1^o \quad (\text{Eq. 16})$$

For the continuous process, the volume of the extraction phases corresponds to the volumetric flow rates inside the reactor, which stay constant during the process and thus Eq. 15 can be rewritten as

$$c_{MeAc,0}^a \dot{V}_a + c_{MeAc,0}^o \dot{V}_o = c_{MeAc,1}^a \dot{V}_a + c_{MeAc,1}^o \dot{V}_o \quad (\text{Eq. 17})$$

The initial concentration $c_{MeAc,0}^a$ before the extraction process is defined as

$$c_{MeAc,0}^a = c_{MeAc,in}^a + c_{HAc,in} X \quad (\text{Eq. 18})$$

which describes the amount of methyl acetate to be distributed between the phases as the sum of the experimental inlet concentration and the amount of methyl acetate produced according to the calculated conversion related to acetic acid or methanol according to the CSTR-cascade model described in section 4.3.1.

Substituting the methyl acetate concentration in the aqueous phase after the reactor $c_{MeAc,1}^a$ with

4 Methods of data evaluation

$$c_{MeAc,1}^a = \frac{c_{MeAc,1}^o}{K} \quad (\text{Eq. 19})$$

and the volumetric flowrate of the organic phase \dot{V}_o via the definition of the phase ratio P by

$$\dot{V}_o = \frac{\dot{V}_a}{P} \quad (\text{Eq. 20})$$

yields after rearrangement and simplification following equation for the methyl acetate concentration in the organic phase after the reactor

$$c_{MeAc,1}^o = \frac{K(c_{MeAc,0}^a P + c_{MeAc,0}^o)}{K+P} \quad (\text{Eq. 21})$$

back substitution of Eq. 19 into Eq. 17 gives after simplification following equation for the methyl acetate concentration in the aqueous phase after the reactor

$$c_{MeAc,1}^a = \frac{(c_{MeAc,0}^a P + c_{MeAc,0}^o)}{K+P} \quad (\text{Eq. 22})$$

4.4 Hold-Up

Dispersed organic phase hold-up was calculated according to [20] by

$$\varepsilon_o = \left(\frac{\Delta P}{g \Delta h (\rho_o - \rho_a)} - \frac{\rho_a}{\rho_o - \rho_a} \right) * 100 \quad (\text{Eq. 23})$$

where ΔP is calculated by the difference between hydrostatic pressure inside the column for pure aqueous phase and differential pressure measured as

$$\Delta P = \rho_a g \Delta h - dP \quad (\text{Eq. 24})$$

In above equations Δh denotes the height difference between the connection points of the differential pressure sensor at the column.

Hold-up of the catalyst is determined by

$$\varepsilon_{cat} = \left(\frac{r^2 \pi \Delta h_{cat} * 0.74}{V_{reactor}} \right) * 100 \quad (\text{Eq. 25})$$

Where Δh_{cat} is determined as described in section 3.2.2. The factor 0.74 [22] stems from the assumed densest packing of the catalyst particles in the sedimentation vessel.

5 Results and discussion

In this section, the results of the calculations are presented and discussed.

5.1 General observations

Stable operation of 3-phase flow (liquid-liquid-solid) inside the TCDC was realized without the addition of air. Reactive extraction experiments conducted by Maier required a fourth gaseous phase for stable operation, a challenge which was overcome. In Fig. 5-1 below, 3-phase flow during reactive extraction is depicted.

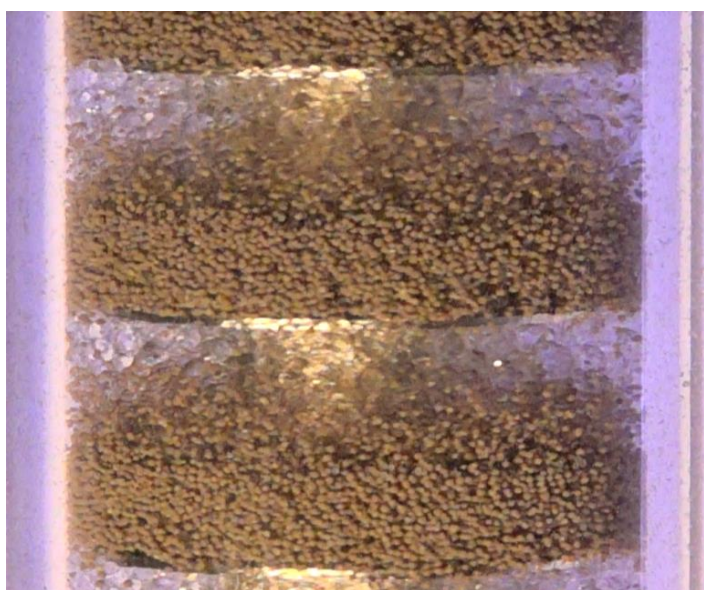


Fig. 5-1: 3-phase flow (liquid-liquid-solid) in the TCDC, system: aqueous/organic/catalyst, photo taken with slow motion camera, $P=1$, $\text{rpm}=650$, $w_{cat}=10.3\%$

As can be seen, the catalyst accumulates in the lower part of the compartments, which was expected. Even at higher rotational speeds this remained the case since the upper part of the compartment is occupied by dispersed organic phase. Concerning movement of phases along the column, both organic liquid phase and catalyst travel along the gap between rotor disc and reactor wall. In some cases, random blockages of compartments with catalyst during start-up of the column were observed, which however always resolved after some minutes and the column transitioned into stationary operation.

5 Results and discussion

The first hour of plant operation cannot be considered as stable, due to temperatures in head and bottom taking time to become constant and volumetric flowrates having to be adjusted in some cases. This is also projected by the differential pressure profile, which was monitored continuously. Shown in Fig. 5-2 below is the differential pressure profile of the experiments used for data analysis and modelling.

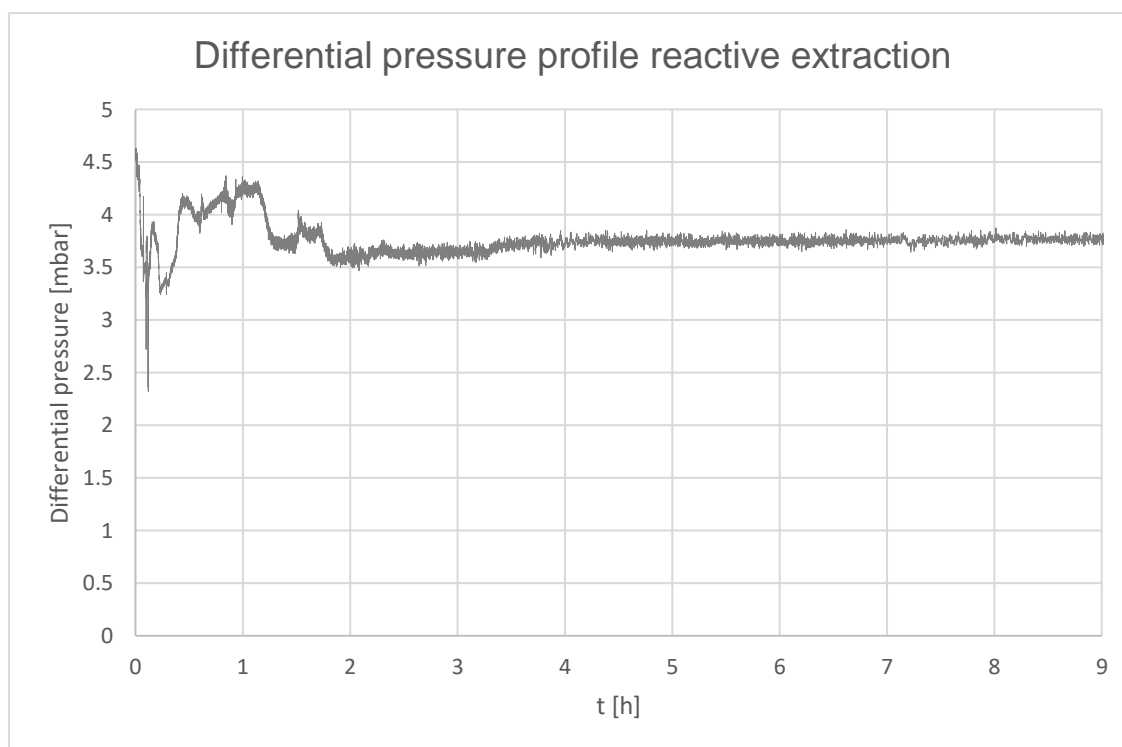


Fig. 5-2: Differential pressure profile of reactive extraction process, mean value of 3 experiments (MN_07, MN_08, MN_09). Parameters: $T = 65\text{ }^{\circ}\text{C}$, $P = 0.5$, rpm = 600

The profile shows, that after the start-up phase, excellent stability for several hours is achieved, until termination (shutdown not included in differential pressure profile) due to no observable change in concentrations which corresponded to reaching equilibrium. For the fitting of the rate constants the first hour of plant operation was not considered. An issue, which was observed after the plant was running for several hours, is the grinding of the catalyst particles by the peristaltic slurry pump. Ultimately this leads to loss of catalyst. Alternative ways of conveying, for instance by external pressurization, are needed to tackle this problem if scale up should be pursued.

5 Results and discussion

The outcome of the gas chromatographic analysis for all compounds of interest in both phases is discussed on the following pages. The diagrams, starting with methyl acetate, are plotted from the mean values of MN_07, MN_08 and MN_09, since these experiments were conducted at the same parameters ($T = 65\text{ }^{\circ}\text{C}$, $P = 0.5$, $\text{rpm} = 600$).

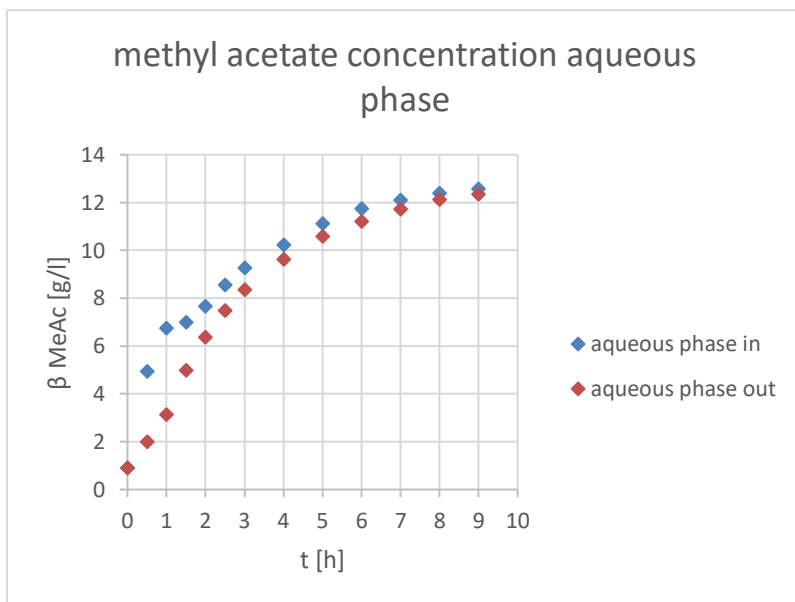


Fig. 5-3: Methyl acetate concentrations in the aqueous phase

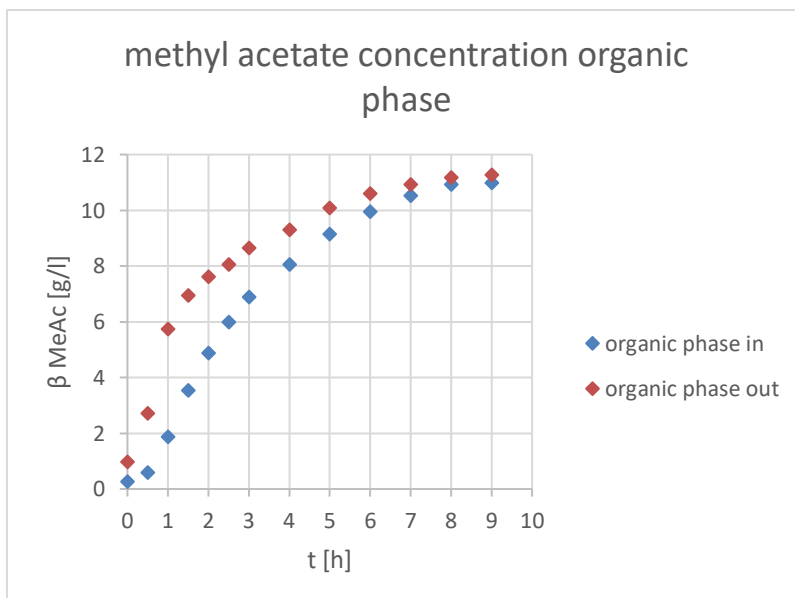


Fig. 5-4: Methyl acetate concentrations in the organic phase

5 Results and discussion

As expected, in the aqueous phase methyl acetate concentration decreases along the column. In contrast, for the organic phase, enrichment takes place along the column and the concentration increases. For both phases, the starting concentration at $t = 0$ does not equal zero (Fig. 5-3, Fig. 5-4), since as reference zero a stable liquid-liquid flow was chosen. Depending on the experiment this point was reached up to 2 hours after preparing the feed solution. Still, this shows that without catalyst the reaction is very slow.

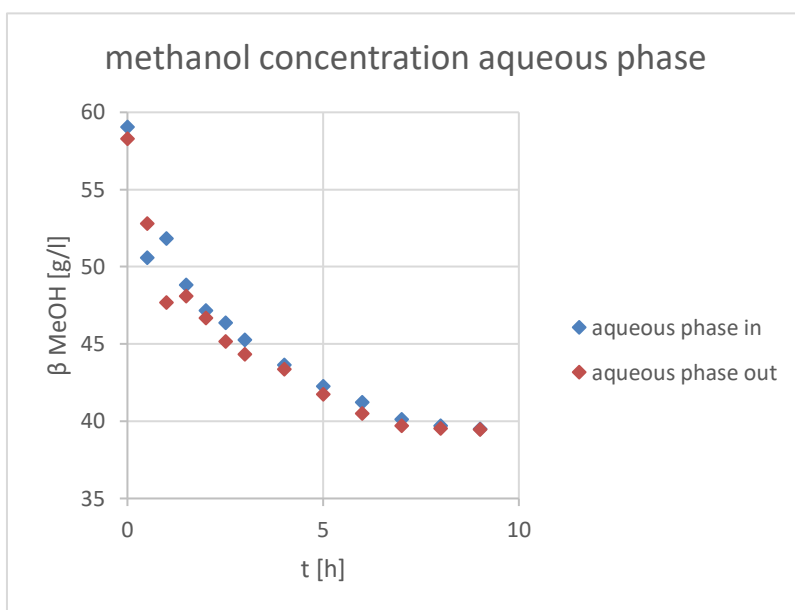


Fig. 5-5: Methanol concentrations in the aqueous phase

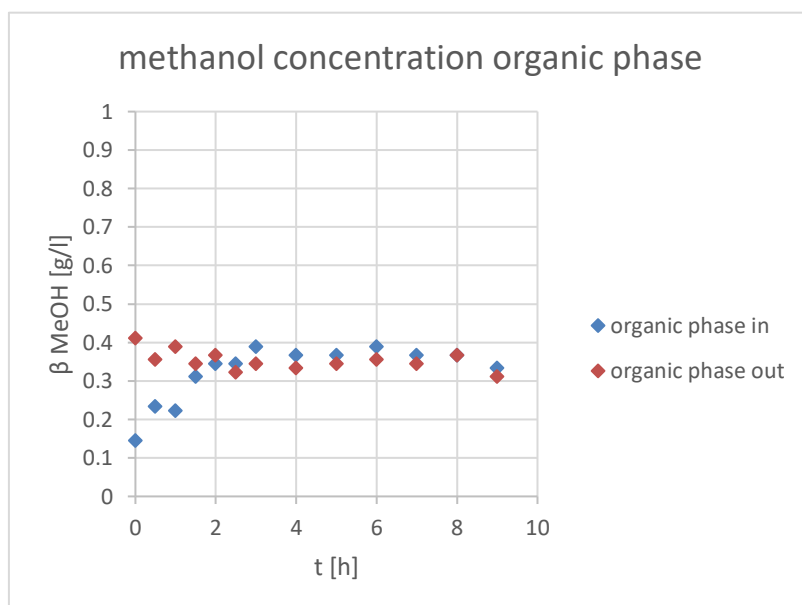


Fig. 5-6: Methanol concentrations in the organic phase

5 Results and discussion

For methanol, in Fig. 5-5 above, a decrease along the column can be observed, which was expected since the esterification reaction takes place. In the organic phase, the methanol concentration reaches a plateau after about 2 hours and then stays constant during the experiment. Compared to the concentration in the aqueous phase, the amount of methanol in the organic phase is minor and thus can be considered insignificant in terms of influencing kinetics or the equilibrium.

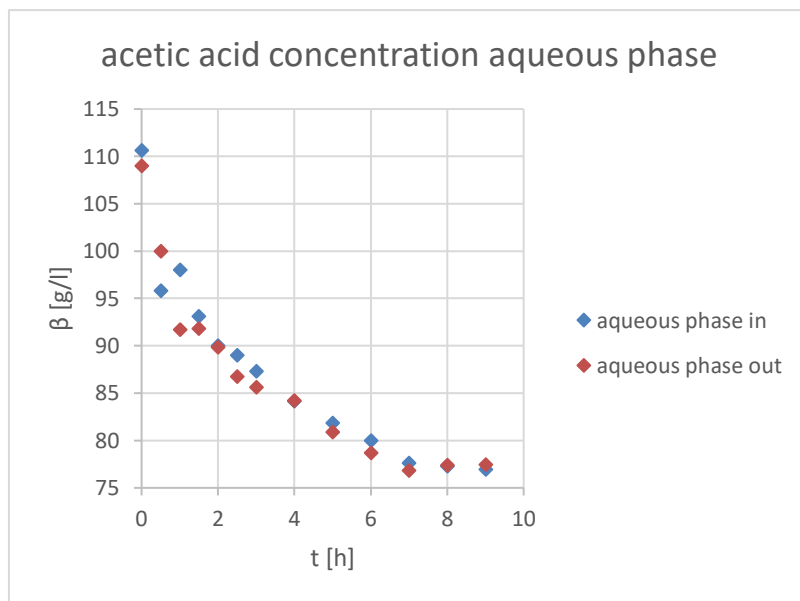


Fig. 5-7: Acetic acid concentrations in the aqueous phase

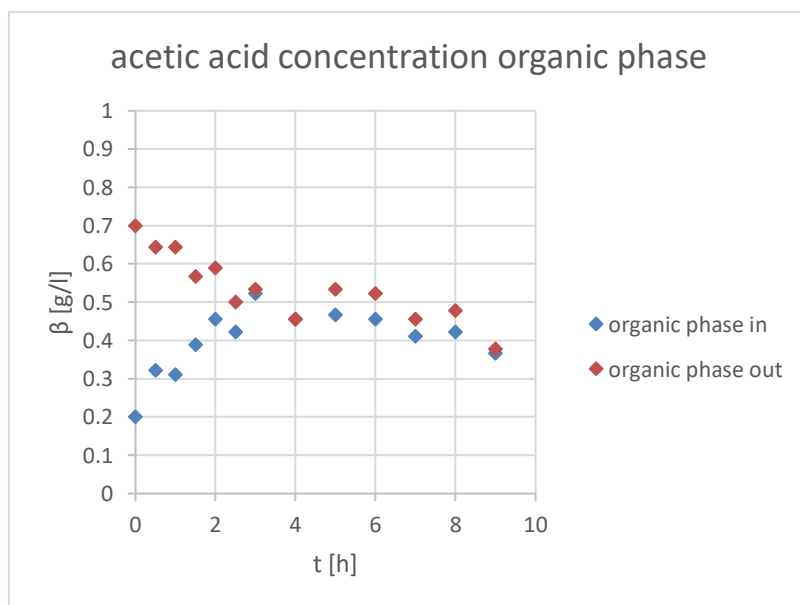


Fig. 5-8: Acetic acid concentrations in the organic phase

For acetic acid, the same trends as for methanol are observed, although the representation of the decrease along the column is not as smooth as for methanol. This is a known issue, with possible causes coming from the analytic side.

5.2 Hold-up results

Hold-up calculations were made for experiments MN_08 and MN_09 ($T = 65\text{ }^{\circ}\text{C}$, $P = 0.5$, $\text{rpm} = 600$) because data was available, and modelling was partly based on these experiments. Densities were determined for the respective phases at 65°C . A blank value for the differential pressure, which was recorded at the column operating without dispersed phase at 65°C , was subtracted from the differential pressure value in liquid-liquid operation at 65°C . This way, errors related to temperature differences between column and reference pipe for the differential pressure sensor were eliminated since the reference pipe could not be heated and brought to the temperature level of the column. The reactor volume for calculation of the catalyst hold-up was defined as the active part of the column, since the largest amount of catalyst was accumulated inside the active part. The amount of catalyst in the inactive part between uppermost compartment and inlet of aqueous phase respectively between lowest compartment and sedimentation vessel is assumed to be not significant in relation to the amount in the active part.

Table 4 below shows the summary of the results.

Table 4: Hold-up values for organic phase and catalyst

	ϵ_o [%]	ϵ_{cat} [%]
MN_08	8.0	4.8
MN_09	8.9	4.4
mean	8.4	4.6

5.3 Influence of phase ratio on conversion

Fig. 5-9 below depicts the conversion of acetic acid for different phase ratios in the quasi-continuous experiments conducted in the TCDC.

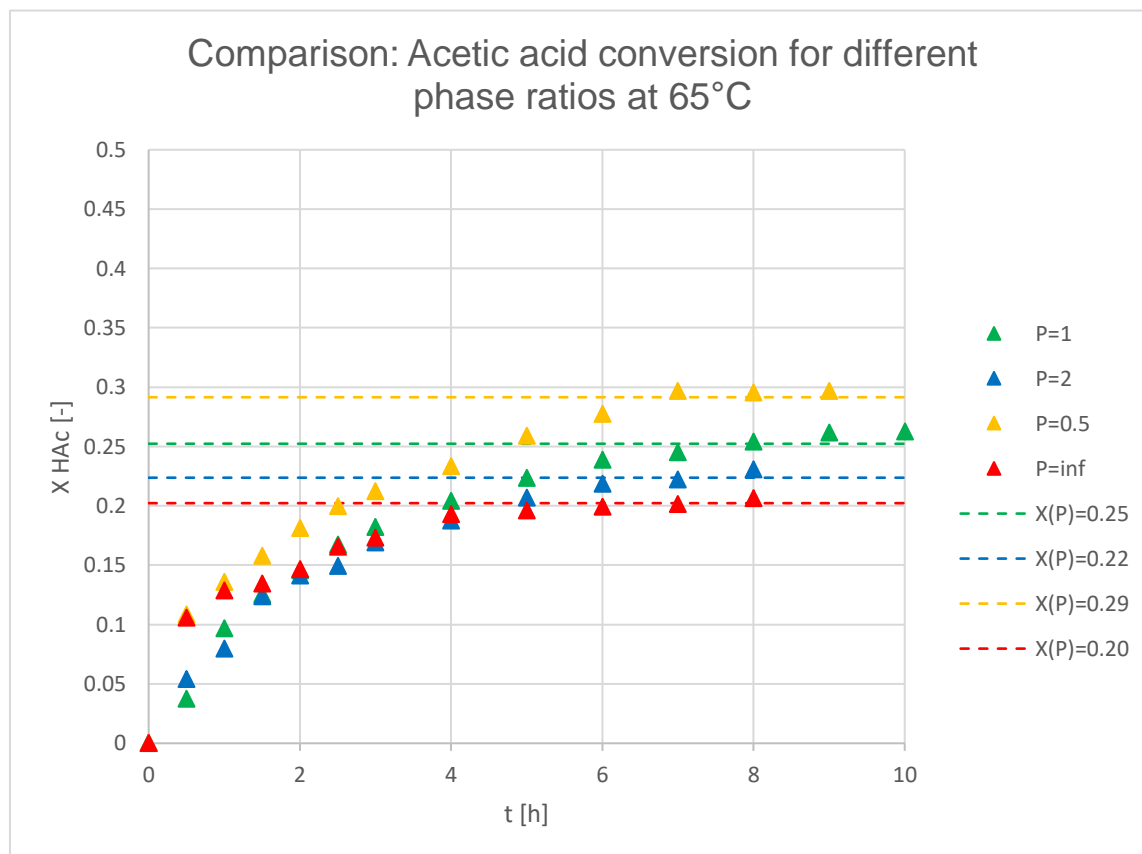


Fig. 5-9: Comparison of conversion with varying phase ratios at 65°C, P=inf --> no extraction, only reaction

As can be seen in the diagram, the final conversion of acetic acid increases for decreasing phase ratio, since more methyl acetate can be extracted into the organic phase which leads to an equilibrium shift according to Le Chatelier. As reference zero, the point of reaching a stable liquid-liquid flow was chosen. Acetic acid was taken as reference compound because its boiling point (b.p. 118 °C, atmospheric pressure) lies well above the process temperature of 65°C. The concentrations used for the calculation of the conversion were defined as the mean of the reactor's inlet and outlet concentration. For the calculation of the final conversion the mean of the values from 6 hours onwards was taken since changes from thereafter are considered to be minor.

5 Results and discussion

Since no batch data for the process temperature of 65 °C is available, comparison with the results produced by Maier can only be done qualitatively. Shown below are the results of batch experiments by Maier for varying phase ratios at a temperature of 80°C.

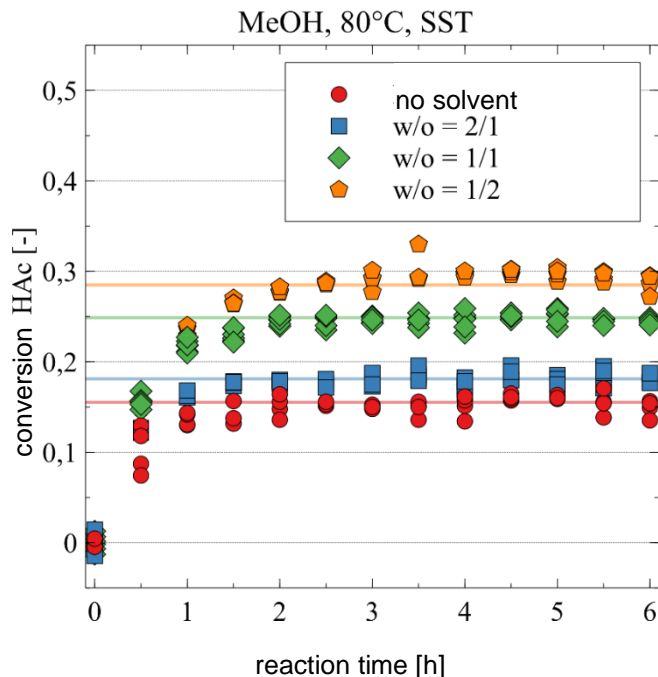


Fig. 5-10: Batch results of reactive extraction at 80°C (system: acetic acid / methanol / Shellsol T) by Maier [3], y-axis: acetic acid conversion, x-axis: time in hours, orange: $P=0.5$, green: $P=1$, blue: $P=2$, red: $P=\infty$

The trend of these batch results matches the findings observed in the quasi-continuous process, although perceptibly lower conversions are achieved at 80°C. This may be explained by the fact that the esterification of acetic acid with methanol is a slightly exothermic reaction ($\Delta H_r = -5.42$ kJ/mol [23]) and thus the equilibrium is shifted to the educt side at higher temperatures.

5.4 Molar process balances

The data used in the models is derived from 3 experiments with the same parameters. To check if the data generated in these experiments can be used in further calculations, molar balances for each sampling point have been established. For this, the molar

5 Results and discussion

streams for each compound (including the water generated in the reaction) in ingoing and outgoing streams have been summed up and the difference between inlet and outlet are calculated. The molar flowrate of water has been set equal to the difference in molar flowrate of methyl acetate since the molar amount of water generated must correspond to the molar amount of methyl acetate generated. All balances are listed in the appendix, representatively one balance is shown in Table 5 below.

Table 5: Molar process balance MN_09 (T = 65 °C, P = 0.5, rpm = 600)

MN_09				
total in- going streams [mol/min]	total out- going streams [mol/min]	Δout-in ab- solute [mol/min]	Δout-in relative [%]	total streams mean [mol/min]
0.205	0.206	0.00160	0.78	0.21
0.181	0.189	0.00820	4.43	0.19
0.188	0.181	-0.00709	-3.85	0.18
0.182	0.184	0.00207	1.13	0.18
0.176	0.183	0.00750	4.17	0.18
0.179	0.181	0.00207	1.15	0.18
0.178	0.176	-0.00178	-1.01	0.18
0.173	0.176	0.00319	1.83	0.17
0.171	0.171	-0.00020	-0.12	0.17
0.170	0.170	-0.00004	-0.03	0.17
0.164	0.167	0.00347	2.10	0.17
0.166	0.166	0.00021	0.13	0.17
0.167	0.169	0.00241	1.44	0.17

The percental differences between inlet and outlet lie in the low single digit range. What can be observed is that in the beginning the total molar count decreases rather sharply, which can be explained by the fact that dead volumes inside the plant filled with air

(e.g., in the storage tanks) are saturated with volatile compounds methyl acetate and methanol. After some hours, slight but insignificant losses are observed since with the used plant setup absolute sealing was not possible.

5.5 Kinetic parameter fit

The kinetic parameters k_1 and k'_2 from Eq.1 were fitted to Eq.5. Calculation was performed in Wolfram Mathematica by combining an ODE-solver with a non-linear fitting procedure. Acetic acid conversion data was taken from Experiments MN_07, MN_08 and MN_09. Mean values over all three experiments were used for the fitting procedure. Defined as reference zero is the conversion 0.5 hours after a stable liquid-liquid-solid flow was reached. The result of the fit is shown in Fig. 5-11 below.

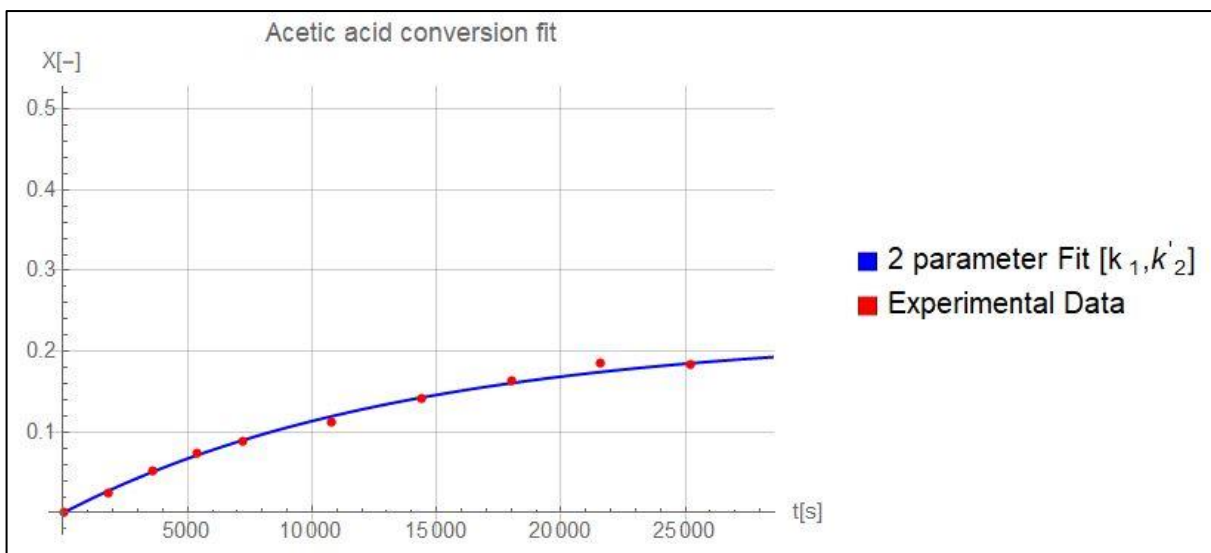


Fig. 5-11: Fit of Eq.5 for rate constants k_1 and k'_2 to experimental data (mean values of MN_07, MN_08 and MN_09)

Table 6 with equation constants and parameter estimates is provided on the next page.

5 Results and discussion

Table 6: Summary and results of the kinetic parameter fit for acetic acid conversion.

Constants	$c_{HAc,0}$ [mol/l]	1.58
	K [-]	0.95
Parameter estimates	k_1 [l/(mol*s)]	$1.0 \cdot 10^{-5}$
	k'_2 [1/s]	$8.5 \cdot 10^{-5}$
relative standard error of parameter estimates	rel. SE k_1 [%]	4.6
	rel. SE k'_2 [%]	11

The value of the distribution coefficient was taken from experimental studies [24]. The fitted rate constants are used in the cascade model as described in section 4.3.1. Batch data would be preferable due to better controllability of the experiments, however kinetic data from Maier was not applicable since different catalyst loadings were used.

5.6 Residence time distribution

As described in section 4.2, two approaches were used for calculation of the number of vessels corresponding to the residence time distribution of the reactor. The results are shown in Fig. 5-12 below.

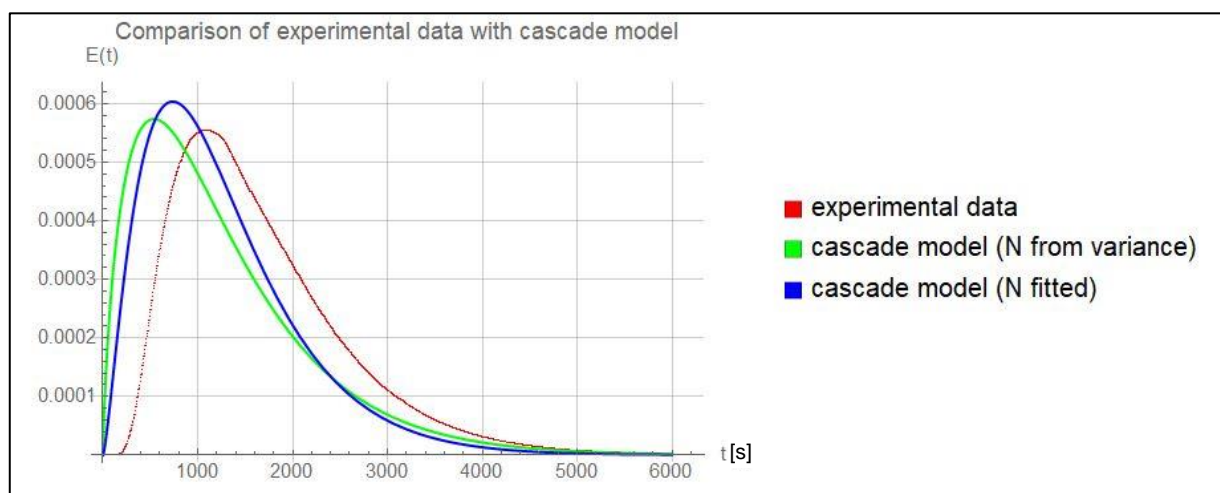


Fig. 5-12: Comparison of experimental data with cascade model

The calculated value of N from the dimensionless variance for a Bodenstein number of 5.9 is 1.7 which corresponds to 2 vessels in practice. The value of N fitted to the exit age distribution is 2.4 which corresponds to 3 vessels in practice. Since the direct fit represents the experimental data better, it was used in further calculations. The experimental residence time as determined in the tracer experiments was 1264 seconds compared to a hydraulic residence time, calculated from the superficial velocity, of 1010 seconds. This difference can be explained by the fact that the actual length of the reactor is shorter than the height difference between tracer injection port and conductivity sensor.

5.7 Modelling of the CSTR cascade

Modelling of the CSTR cascade was done as described in section 4.3.1. Concentration data of methanol was used as input for the conversion calculations since the representation of the decrease along the column was smoother than that of acetic acid. The volatility of methanol is not an issue in this case because from inlet sample port to outlet sample port, the aqueous phase had no contact to the surroundings. The regressed concentration profiles of methanol for inlet and outlet of the reactor are shown below. Like in the kinetic fit, the start-up phase was not included due to instabilities in concentrations and temperatures.

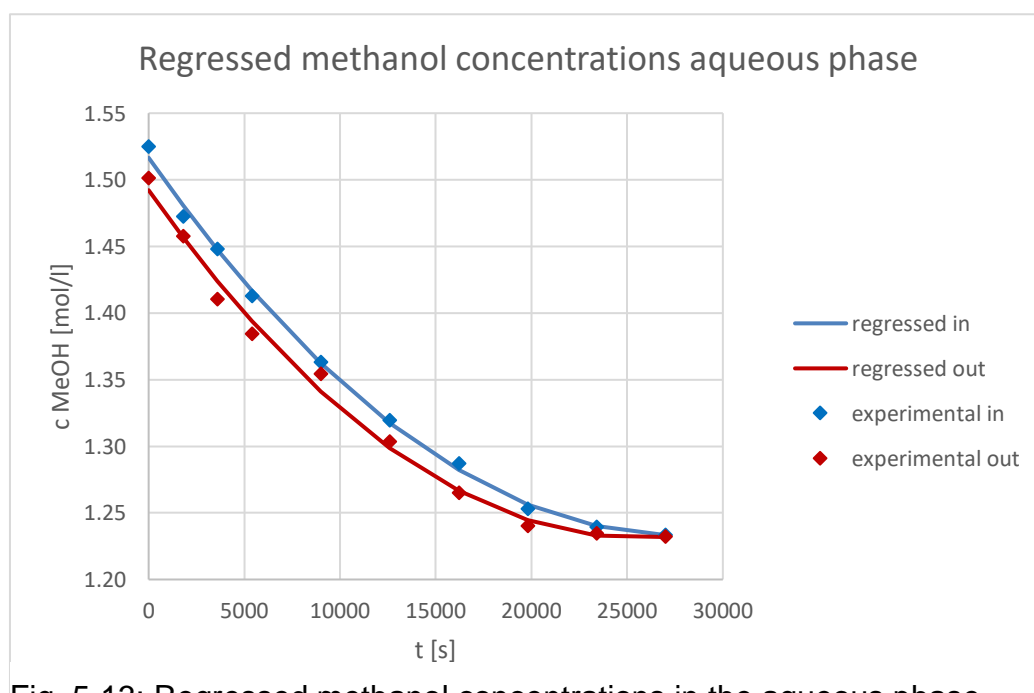


Fig. 5-13: Regressed methanol concentrations in the aqueous phase

5 Results and discussion

Fig. 5-13 shows converging curves for the methanol concentrations in inlet and outlet. Equilibrium is reached eventually and no change along the column is observed anymore. Also, the concentration difference between inlet and outlet decreases with experimental duration as expected, since the reaction rate decreases.

The next figure shows the comparison between regressed outlet values and model values. Input for the model are 3 tanks in series and both experimental as well as hydrodynamic residence time.

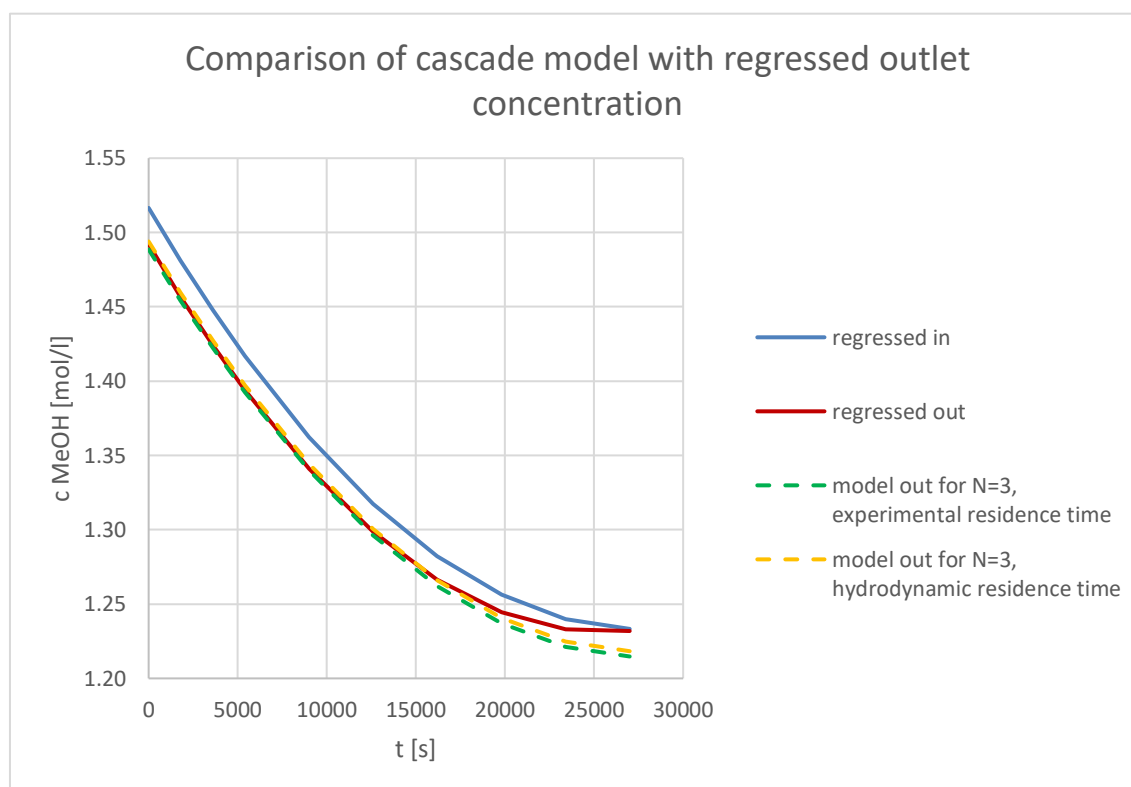


Fig. 5-14: Comparison of cascade model with regressed values

Excellent conformity of the model with experimental data is observed in the initial two thirds of the experiment, with the deviation getting larger towards the end. The converging of the concentration profiles is not depicted by the model. This deviation can be rationalized by taking a closer look at the model input. Input parameters are the initial concentration of methanol and the distribution coefficient. No information about reaction progress is included, and thus the model cannot depict the experimental reality towards equilibrium. However, this is not necessary since the main interest lies in the ability to provide a model for an actual continuous process where the feed solution

5 Results and discussion

is not refed to the reactor and fresh unloaded solvent is used. The difference of the results between experimental and hydrodynamic residence time is minor, and like expected, the outlet concentration is higher (respectively the conversion lower) for smaller residence time inside the reactor.

To depict the experimental reality better towards equilibrium, the rate law was modified. The basic rate law for the esterification reaction is

$$-r_{MeOH} = -\frac{dc_{MeOH}}{dt} = k_1 c_{HAc} c_{MeOH} - k_2 c_{MeAc} c_{H_2O} \quad (\text{Eq. 26})$$

which, utilizing conversion for equimolar starting concentrations of acetic acid and methanol and defining the concentration of water as constant, can be rewritten as

$$-r_{MeOH} = -\frac{dc_{MeOH}}{dt} = k_1 c_{MeOH,0}^2 (1 - X)^2 - k'_2 c_{MeAc} \quad (\text{Eq. 27})$$

The reaction progress is incorporated via Eq. 22 by substituting c_{MeAc} in Eq. 27, which yields

$$-r_{MeOH} = -\frac{dc_{MeOH}}{dt} = k_1 c_{MeOH,0}^2 (1 - X)^2 - k'_2 \frac{(c_{MeAc,0}^a)^P + c_{MeAc,0}^o}{K+P} \quad (\text{Eq. 28})$$

Now the reaction progress is integrated by $c_{MeAc,0}^a$ which is defined as

$$c_{MeAc,0}^a = c_{MeAc,in}^a + c_{HAc,in} X \quad (\text{Eq. 18})$$

and by $c_{MeAc,0}^o$. Both $c_{MeAc,0}^a$ and $c_{MeAc,0}^o$ take into account the methyl acetate in the system in aqueous respectively organic phase before the extraction step and before the reaction.

The result for the cascade model with Eq. 28 as rate law is shown in Fig. 5-15 on the next page. All parameters for the calculation were held constant as in the original model, the only difference was the addition of the phase ratio as an additional parameter. It can be observed that the extended model depicts the experimental reality towards equilibrium more adequately. However, the deviation from regressed values in the far from equilibrium range is larger than the deviation of the original model used. The main reason for this is supposed to be inaccuracies related to the rate constants. The rate constants were fitted to data of a process in a technical apparatus, were accurate parameter control, as needed for kinetic experiments in general, is difficult.

5 Results and discussion

Therefore, it is highly recommended for future research to determine the rate constants in controlled batch experiments for the according process parameters to get better results.

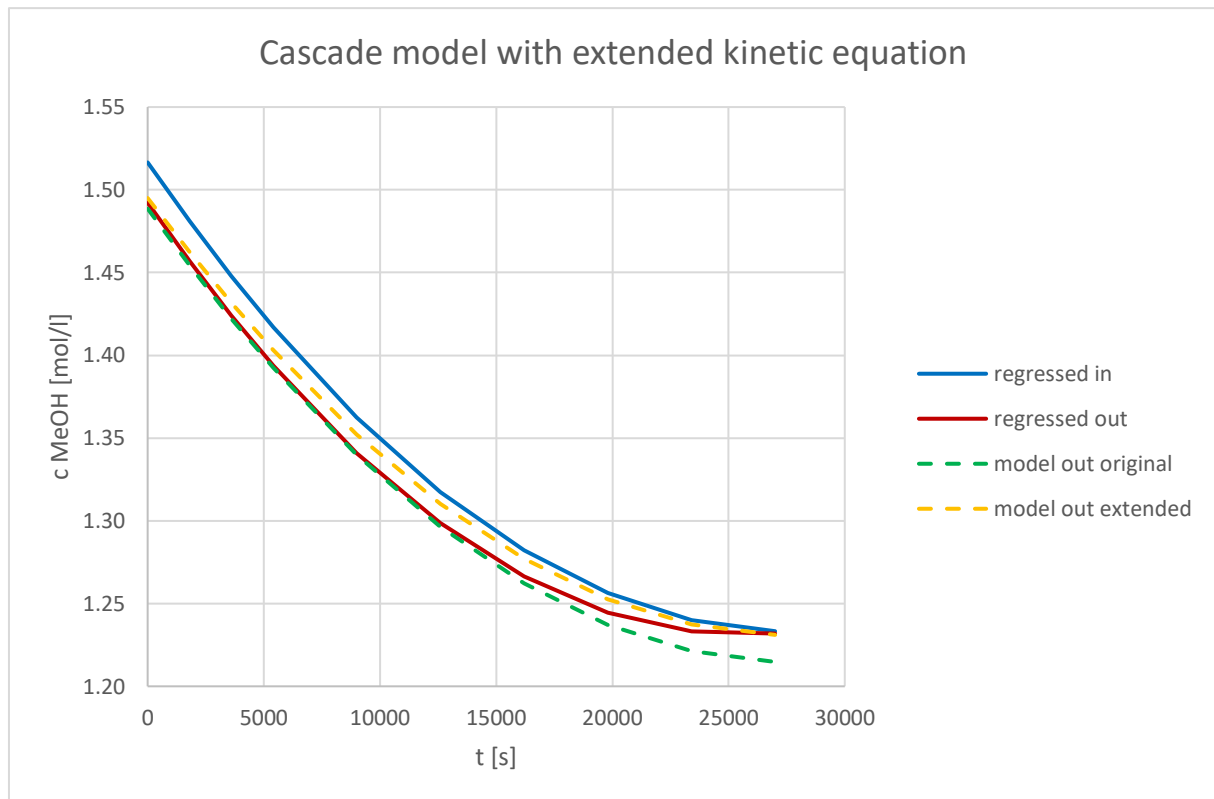


Fig. 5-15: Cascade model with extended kinetic equation

Another source of error is the slow kinetics of the reaction, which leads to small concentration differences for the reactants between inlet and outlet. Sampling or analysis errors thus have a much more severe impact on the results.

5.8 Modelling of methyl acetate concentrations

Since the methyl acetate concentrations in both phases are not only based on kinetics but also on distribution laws, the cascade model alone is not sufficient. A simple model based on Nernst distribution was developed as described in section 4.3.2. Comparison of methyl acetate concentrations in the aqueous phase outlet between experimental data and model is shown in Fig. 5-16 below. Like in previous sections, the start-up phase was not considered. Conversion values were taken from the cascade model.

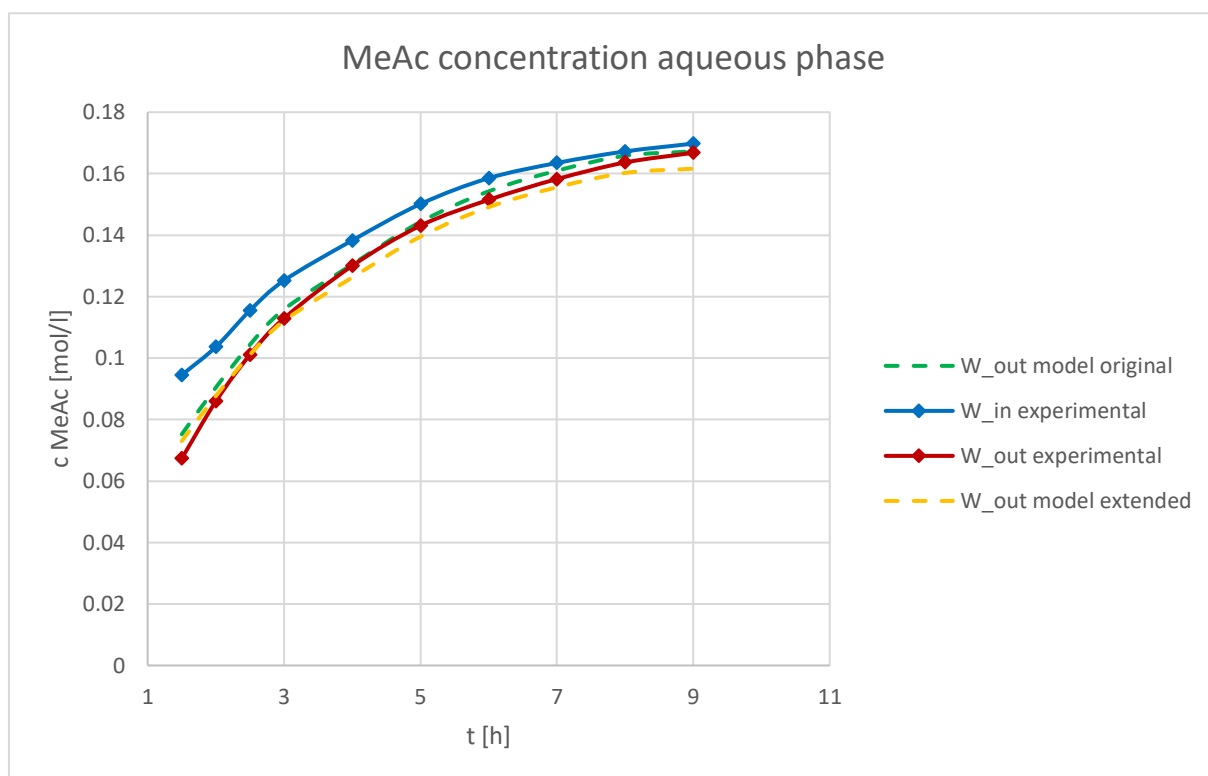


Fig. 5-16: Comparison of methyl acetate concentrations in the aqueous phase, model parameters: $K = 0.95$, $P = 0.5$

Both models show good conformity with the experimental values. For the extended model, the concentrations towards equilibrium are lower because the conversion is also lower, as depicted in Fig. 5-15. Since this distribution model builds on the cascade model, the validity of latter is further supported.

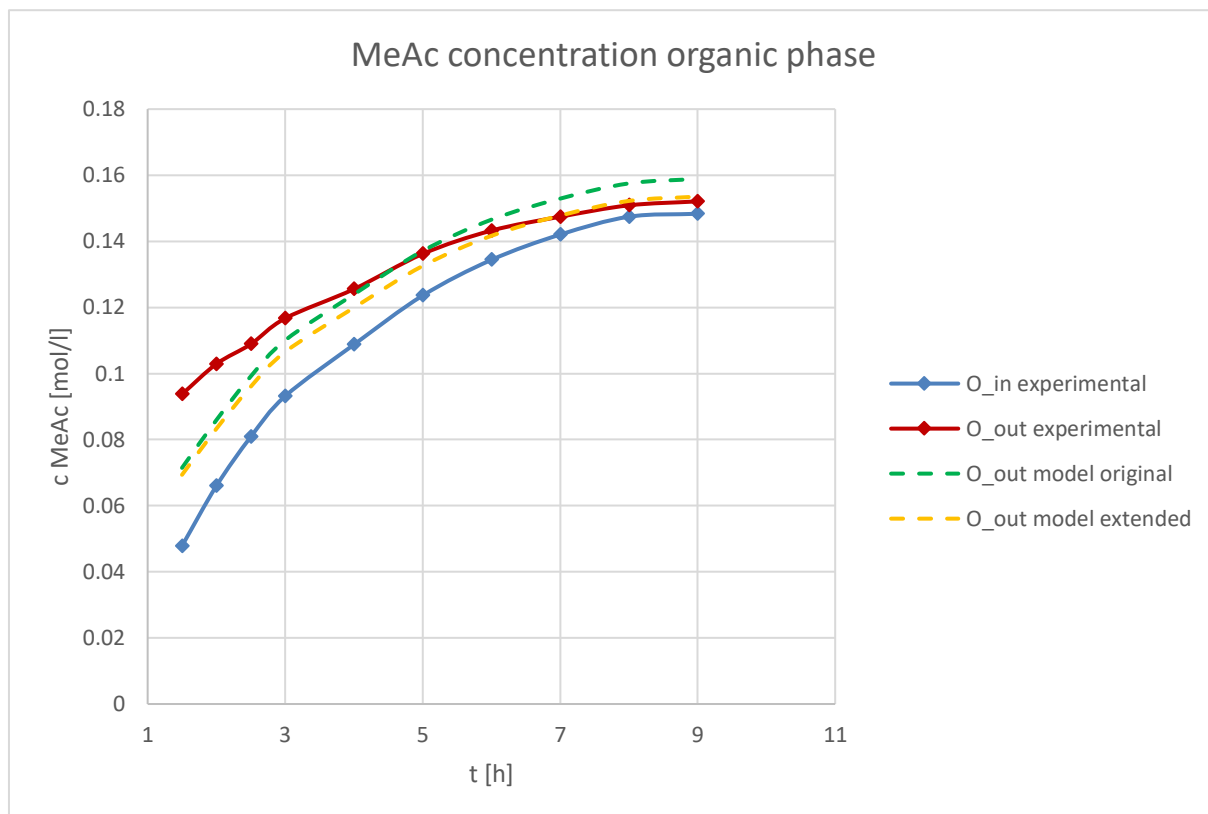


Fig. 5-17: Comparison of methyl acetate concentrations in the organic phase, model parameters: $K = 0.95$, $P = 0.5$

The methyl acetate concentrations in the organic phase are not depicted as accurately as the methyl acetate concentrations in the aqueous phase by the original model. The deviation towards the end can be explained by the fact that the predicted conversions are higher than the experimental values. However, for the extended model, the conformity of the extended model towards equilibrium is better. Further error sources can be related to sampling (since sampling probe had a fixed length and samples could not always be taken directly at the phase boundary) and volatility of methyl acetate (here being a problem because the organic phase had more contact to surroundings at column head, also at higher temperatures)

5.9 Scale up calculation

The established model is exemplarily applied to a theoretical scale up of the reactor. Following assumptions are made:

- Scale up of the reactor is only done in height, not in diameter

5 Results and discussion

- The number of vessels per length of reactor is defined as constant
- The number of vessels in the cascade is scaled linearly with the height of the reactor
- Only the active part of the column (compartments) is scaled up, therefore the hydrodynamic residence time is used in the calculation
- To compensate for possible deviations caused by the usage of the hydrodynamic residence time, for the original reactor the number of vessels is set to $N = 2$ as a safety factor
- The feed is not refeed into the reactor and fresh unloaded solvent is used
- The extraction is treated as single-step

The parameters of the scaled-up reactor are listed below in Table 7.

Table 7: parameters for scaled up reactor

active height [m]	6
number of vessels according to cascade model [-]	20
residence time [s]	10100

The calculation is done in the same way as for the experiments, just with different values. The original model was used. For the continuous case, the initial concentration of methyl acetate in aqueous and organic phase ingoing streams is set to zero. All other parameters (k_1 , k'_2 , K , P) have been held constant. The starting concentration for acetic acid is set to 2 mol/l.

5 Results and discussion

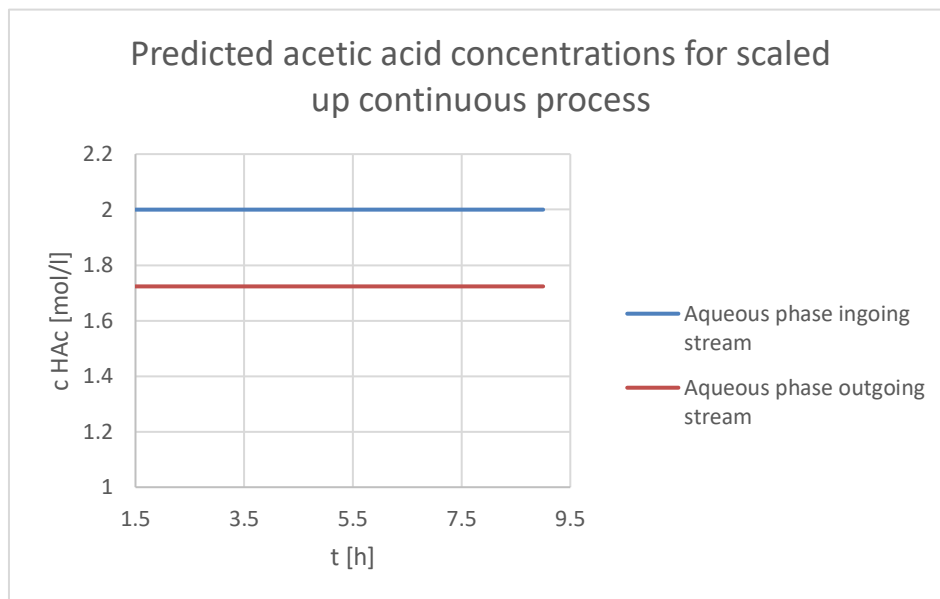


Fig. 5-18: Predicted acetic acid concentrations for scaled up process

The model predicts a conversion of 0.138, lowering the initial concentration from 2 mol/l to 1.72 mol/l. Related to the outlet concentration of the solvent phase, this means that 9% of the acetic acid in the feed stream can be removed. The results for methyl acetate are shown below.

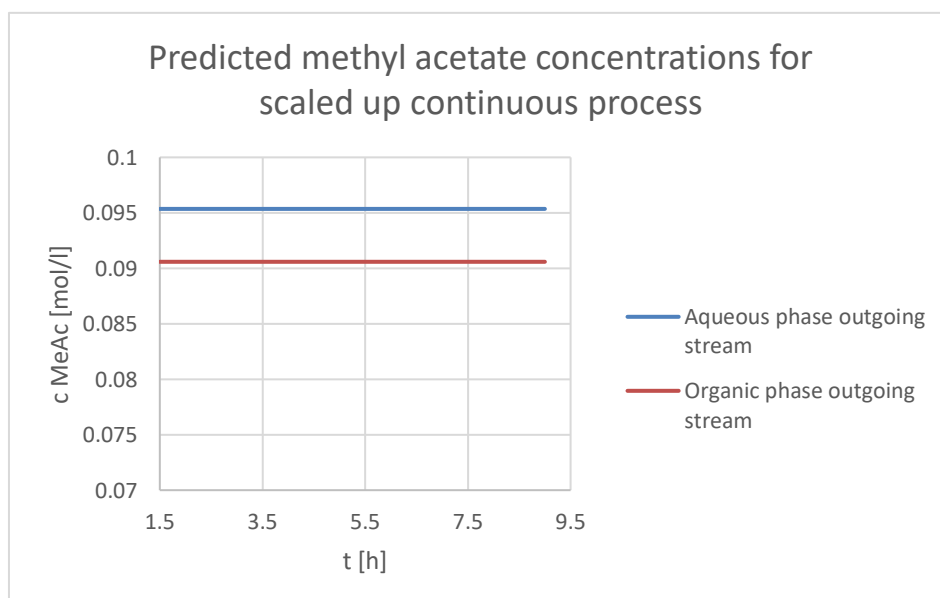


Fig. 5-19: Predicted methyl acetate concentrations for scaled up process

5 Results and discussion

It becomes apparent that the solvent used is not the optimal choice, since 34% of the methyl acetate produced leaves the reactor with the aqueous phase. This value drops by 41% to 20% for a hypothetical distribution coefficient of $K = 2$ via a rough estimate only considering distribution and no influence of distribution coefficient on conversion, which shows that there is definitely room for improvement.

6 Summary and Outlook

The focus of this thesis lay on experimental studies and modelling of reactive extraction in a Taylor-Couette-Disc-Contactor. Basis for the work was a proof of concept for the heterogeneous catalytic reactive extraction of acetic acid from aqueous feeds by Maier [3]. The existing plant was modified to improve the quality of results. Operation was achieved without the addition of a fourth gaseous phase (air), which was previously needed for a stable process, reducing the complexity and effort from the apparatus point of view. A differential pressure sensor was used to monitor the process permanently by measuring the differential pressure between head and bottom of column, which corresponds to the phase holdup inside the column. Experiments in the Taylor-Couette-Disc-Contactor were carried out at different phase ratios and the results compared with the batch results of Maier. Although direct comparison was not possible because of different temperatures and catalyst loadings used in the batch experiments, the trend was confirmed. The conversion increases for decreasing phase ratio, as more methyl acetate can be removed into the organic phase, and the equilibrium can be shifted according to Le Chatelier's principle. Process balances were established for the experiments used in the calculations, comparing the total molar ingoing streams for the compounds of interest (acetic acid, methanol, methyl acetate, water produced in the reaction) with the total molar outgoing streams. Differences were in the low single digit range. The kinetic parameters for the esterification were retrieved by fitting the differential conversion form of the rate law to experimental acetic acid conversion data. Residence time distribution measurements for the reactor via pulse function tracer experiments were made. A saturated sodium chloride solution was used as tracer, the output signal was detected by a conductivity sensor. A routine programmed in LabView by Preisack [19] was used for determination of the axial dispersion coefficient. This coefficient was then used to calculate the Bodenstein number of the reactor, and from this the number of vessels of an equivalent continuous-stirred-tank-reactor cascade via the dimensionless variance for the open-open case. Another approach to obtain the equivalent number of vessels was a direct fit of the exit age distribution of a CSTR-cascade to experimental data. The value from latter was used for the modelling of the cascade. The final conversion in the aqueous phase for the cascade model was ob-

tained from stepwise and numeric solution of the design equation. Fitted rate constants, as described above, were used in the calculation. As input for initial concentrations, regressed values from experimental data of methanol inlet concentrations were used. Methanol was chosen because the concentration profiles are smoother compared to acetic acid. The reason for this is supposed to be on the analytic side, which was however not investigated. The volatility of methanol at process temperatures posed no problem in this case since there was no contact of aqueous phase and surroundings between sampling points. The model showed good conformity with experimental data in the first thirds of the experiment. Towards equilibrium, the original model is not able to describe reality of the experiment since no information about reaction progress is included in the kinetic equation. The model was extended by taking initial product concentrations in both aqueous and organic phase into account. Through this, it was possible to describe the concentration curves towards equilibrium. For the organic phase, a simple model based on Nernst distribution was developed, in which the conversion of methanol in the aqueous phase obtained from the cascade model was used. The distribution model reflects the concentration profile in the aqueous phase well. However, the deviations of the experimental concentrations from the model in the organic phase are larger. Possible error sources include sampling, organic phase contact to the surroundings and model conversion being higher than the experimentally observed ones towards the end of the experiment. Exemplarily a theoretical scale up was presented. For a column with an active height of 6 m and the same diameter of 50 mm the predicted conversion of acetic acid is 14%. Regarding future research on the topic, validation of the results by further experimental data possibly in scale up and refining of the kinetic model, including the determination of the rate constants in batch experiments for different catalyst loadings, will be further steps towards being fully able to describe this complex process accurately. Solvent screening and testing will be important to improve the efficiency and thus the economics of the process. Higher process temperatures are worth considering since the kinetics at 65 °C are still rather slow. Studies on solvent recycling are also needed if the technical application of this process is pursued. At last, it shall be noted that the continuous reactive extraction process in the Taylor-Couette-Disc-Contactor is certainly not limited to esterification, and especially viable in view of reactions with faster kinetics.

7 Literature

- [1] Painer, D.; Lux, S.; Graftschafter, A.; Toth, A.; Siebenhofer, M. Isolation of carboxylic acids from biobased feedstock. *Chemie-Ingenieur-Technik* **2017**, *89* (1), 161–171. <https://doi.org/10.1002/cite.201600090>.
- [2] Naqvi, M.; Yan, J.; Dahlquist, E. Black liquor gasification integrated in pulp and paper mills: A critical review. *Bioresour. Technol.* **2010**, *101* (21), 8001–8015. <https://doi.org/10.1016/j.biortech.2010.05.013>.
- [3] Maier, T. Verfahrensentwicklung einer kontinuierlichen heterogen katalysierten Veresterung mit zeitgleicher Produktextraktion, TU Graz, Master Thesis, 2020.
- [4] Van Gerven, T.; Stankiewicz, A. Structure, Energy, Synergy, Time—the Fundamentals of Process Intensification. *Ind. Eng. Chem. Res.* **2009**, *48* (5), 2465–2474. <https://doi.org/10.1021/ie801501y>.
- [5] Keil, F. J. Process Intensification. *Rev. Chem. Eng.* **2018**, *34* (2), 135–200. <https://doi.org/10.1515/revce-2017-0085>.
- [6] Mersmann, A.; Kind, M.; Stichlmair, J. Extraktion. In *Thermische Verfahrenstechnik*; Chemische Technik / Verfahrenstechnik; Springer-Verlag: Berlin/Heidelberg, 2005; pp 345–376. <https://doi.org/10.1007/3-540-28052-9>.
- [7] Rauber, J. Design practice for packed liquid liquid extraction columns. *AIChE Annu. Meet. Conf. Proc.* **2006**.
- [8] Aksamija, E. Der Taylor-Couette Disc Contactor (TCDC); Ein vereinfachtes end optimiertes Design von Drehscheibenextraktoren, TU Graz, PhD Thesis, 2014.
- [9] Aksamija, E.; Weinländer, C.; Sarzio, R.; Siebenhofer, M. The Taylor-Couette Disc Contactor: A novel apparatus for liquid/liquid extraction. *Sep. Sci. Technol.* **2015**, *50* (18), 2844–2852. <https://doi.org/10.1080/01496395.2015.1085406>.
- [10] Graftschafter, A.; Aksamija, E.; Siebenhofer, M. The Taylor-Couette Disc Contactor. *Chem. Eng. Technol.* **2016**, *39* (11), 2087–2095. <https://doi.org/10.1002/ceat.201600191>.
- [11] Graftschafter, A.; Siebenhofer, M. Design rules for the Taylor-Couette Disc Contactor. *Chemie-Ingenieur-Technik* **2017**, *89* (4), 409–415. <https://doi.org/10.1002/cite.201600142>.
- [12] Scott Fogler, H. *Elements of Chemical Reaction Engineering*, 5th ed.; Prentice Hall, 2016.
- [13] Xu, Z. P.; Chuang, K. T. Kinetics of acetic acid esterification over ion exchange catalysts. *Can. J. Chem. Eng.* **1996**, *74* (4), 493–500. <https://doi.org/10.1002/cjce.5450740409>.
- [14] Lux, S.; Winkler, T.; Berger, G.; Siebenhofer, M. Kinetic study of the heterogeneous catalytic esterification of acetic acid with methanol using Amberlyst®15. *Chem. Biochem. Eng. Q.* **2015**, *29* (4), 549–557. <https://doi.org/10.15255/CABEQ.2014.2083>.
- [15] Pöpken, T.; Götze, L.; Gmehling, J. Reaction kinetics and chemical equilibrium of homogeneously and heterogeneously catalyzed acetic acid esterification with

- methanol and methyl acetate hydrolysis. *Ind. Eng. Chem. Res.* **2000**, 39 (7), 2601–2611. <https://doi.org/10.1021/ie000063q>.
- [16] Dumesic, J. A.; Huber, G. W.; Boudart, M. Principles of heterogeneous catalysis. In *Handbook of Heterogeneous Catalysis*; Wiley-VCH Verlag GmbH & Co. KGaA: Weinheim, Germany, 2008. <https://doi.org/10.1002/9783527610044.hetcat0001>.
- [17] Bart, H.-J. *Reactive Extraction*; Springer, Berlin, Heidelberg, 2001. https://doi.org/10.1007/978-3-662-04403-2_1.
- [18] Bart, H.-J. Reactive Extraction In Stirred Columns – A Review. *Chem. Eng. Technol.* **2003**, 26 (7), 723–731. <https://doi.org/10.1002/ceat.200306102>.
- [19] Preisack, B. Aufbau und Inbetriebnahme einer 150mm RDC Kolonne und Entwicklung eines Mess- und Auswertungssystems zur Ermittlung der Verweilzeitverteilung, TU Graz, Master Thesis, 2016.
- [20] Liegl, M. Installation und Inbetriebnahme von Drucksensoren für die Holdup Messung in einem TCDC, TU Graz, Bachelor Thesis, 2020.
- [21] Siebenhofer, M.; Lux, S.; Painer, D. *Chemical Reaction Engineering II - Lecture Script*, 2019.
- [22] Hales, T. C. A Proof of the Kepler Conjecture. *Ann. Math.* **2005**, 162 (3), 1065–1185. <https://doi.org/10.4007/annals.2005.162.1065>.
- [23] Sert, E.; Atalay, F. S. Esterification of acetic acid with methanol over a cation exchange resin. *Prog. React. Kinet. Mech.* **2011**, 36 (3), 239–251. <https://doi.org/10.3184/146867811X13095333117417>.
- [24] Zandt, P. Work in Progress, Expected Publication Date: 2021, TU Graz, Bachelor Thesis.
- [25] Dittmeyer, R.; Emig, G. Simultaneous Heat and Mass Transfer and Chemical Reaction. In *Handbook of Heterogeneous Catalysis*; Wiley-VCH Verlag GmbH & Co. KGaA: Weinheim, Germany, 2008. <https://doi.org/10.1002/9783527610044.hetcat0094>.

8 Appendix

8.1 Pump calibration curves

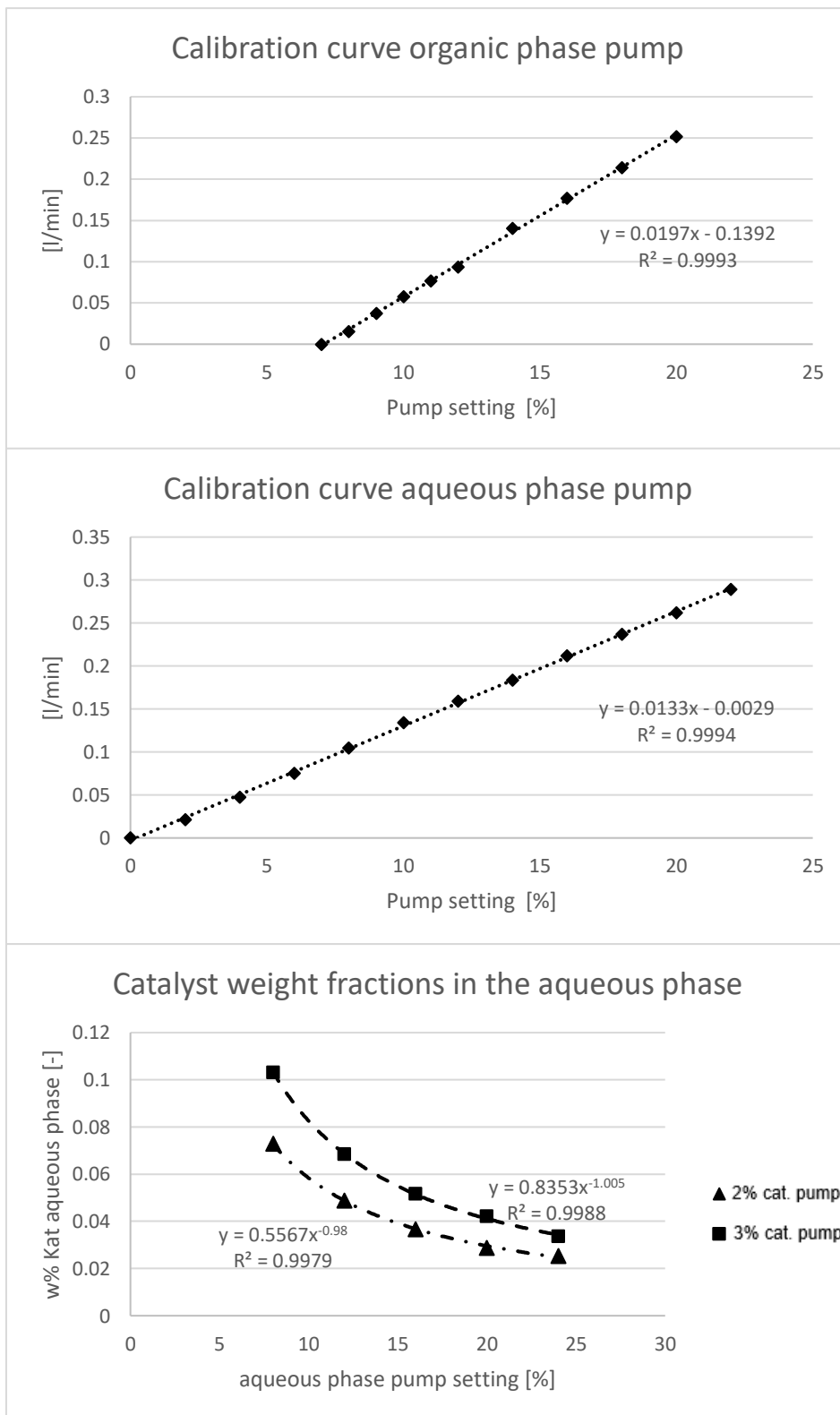


Fig. 8-1: Pump calibration curves

8.2 Process Balances

Table 8: Process balance MN_07

MN_07					
t [h]	total ingoing streams [mol/min]	total out-going streams [mol/min]	Δ out-in absolute [mol/min]	Δ out-in relative [%]	total streams mean [mol/min]
0	0.193	0.193	0.00016	0.08	0.19
0.5	0.165	0.182	0.01692	9.76	0.17
1	0.175	0.169	-0.00591	-3.44	0.17
1.5	0.169	0.173	0.00431	2.52	0.17
2	0.167	0.169	0.00288	1.71	0.17
2.5	0.164	0.163	-0.00115	-0.70	0.16
3	0.163	0.163	0.00044	0.27	0.16
4	0.160	0.163	0.00235	1.46	0.16
5	0.159	0.158	-0.00068	-0.43	0.16
6	0.157	0.155	-0.00165	-1.06	0.16
7	0.154	0.152	-0.00216	-1.41	0.15
8	0.152	0.154	0.00125	0.81	0.15
9	0.151	0.152	0.00075	0.49	0.15

Table 9: Process balance MN_08

MN_08					
t [h]	total ingoing streams [mol/min]	total out-going streams [mol/min]	Δ out-in absolute [mol/min]	Δ out-in relative [%]	total streams mean [mol/min]
0	0.199	0.200	0.00080	0.40	0.20
0.5	0.181	0.184	0.00347	1.90	0.18
1	0.185	0.179	-0.00621	-3.41	0.18
1.5	0.176	0.182	0.00583	3.25	0.18
2	0.176	0.180	0.00388	2.18	0.18
2.5	0.174	0.173	-0.00079	-0.46	0.17
3	0.173	0.175	0.00189	1.09	0.17
4	0.170	0.170	0.00016	0.10	0.17
5	0.166	0.167	0.00104	0.62	0.17
6	0.164	0.162	-0.00224	-1.37	0.16
7	0.164	0.160	-0.00375	-2.31	0.16
8	0.163	0.162	-0.00084	-0.52	0.16
9	0.162	0.161	-0.00080	-0.49	0.16